Article

Cell Reports

TET2 Regulates Mast Cell Differentiation and Proliferation through Catalytic and Non-catalytic Activities

Graphical Abstract

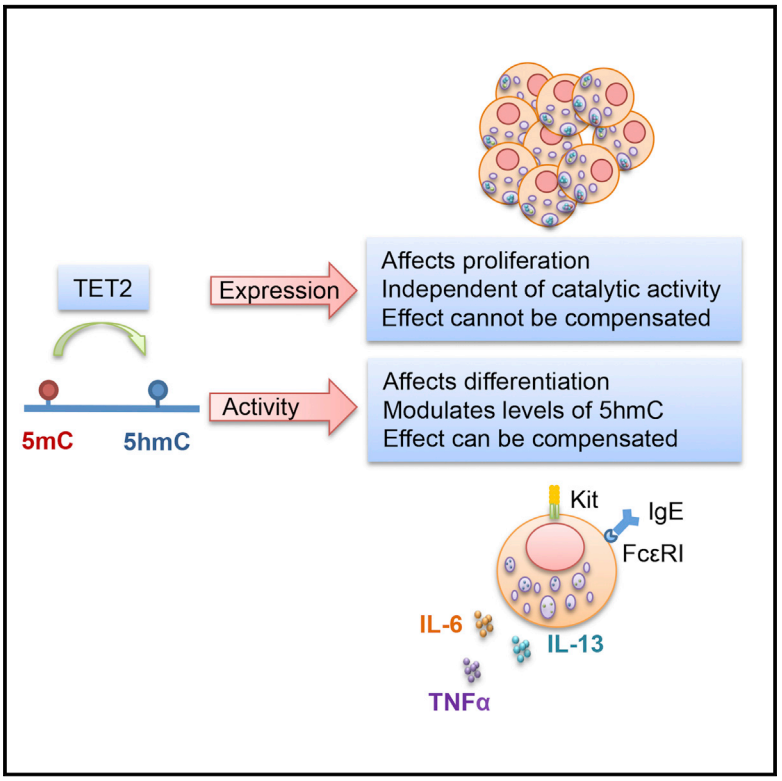

Authors

Sara Montagner, Cristina Leoni, Stefan Emming, ..., Anjana Rao, Gioacchino Natoli, Silvia Monticelli

Correspondence

silvia.monticelli@irb.usi.ch

In Brief

The impact of TET enzymes on gene expression and cell function is incompletely understood. Montagner et al. investigate the TET-mediated regulation of mast cell differentiation and function, uncover transcriptional pathways regulated by TET2, and identify both enzymatic activity-dependent and -independent functions of TET2.

Highlights

- TET2 regulates mast cell differentiation, cytokine production, and proliferation
- Lack of TET2 leads to extensive changes in transcriptome and 5hmC landscape
- Cell differentiation defects can be compensated for by other TETs
- Cell proliferation depends on TET2 expression, independent of its enzymatic activity

Accession Numbers

GSE77845

Montagner et al., 2016, Cell Reports *15*, 1566–1579
May 17, 2016
http://dx.doi.org/10.1016/j.celrep.2016.04.044

OPEN ACCESS
CellPress

Cell Reports
Article

TET2 Regulates Mast Cell Differentiation and Proliferation through Catalytic and Non-catalytic Activities

Sara Montagner,[1,2] Cristina Leoni,[1,2] Stefan Emming,[1,2] Giulia Della Chiara,[3] Chiara Balestrieri,[3] Iros Barozzi,[3] Viviana Piccolo,[3] Susan Togher,[4] Myunggon Ko,[4,5] Anjana Rao,[4] Gioacchino Natoli,[3] and Silvia Monticelli[1,*]

[1]Institute for Research in Biomedicine, Universita' della Svizzera italiana (USI), 6500 Bellinzona, Switzerland
[2]Graduate School for Cellular and Biomedical Sciences, University of Bern, 3012 Bern, Switzerland
[3]Department of Experimental Oncology, European Institute of Oncology (IEO), 20139 Milan, Italy
[4]La Jolla Institute for Allergy and Immunology, La Jolla, CA 92037, USA
[5]School of Life Sciences, Ulsan National Institute of Science and Technology, UNIST-gil 50, Ulju-gun, Ulsan 689-798, Republic of Korea
*Correspondence: silvia.monticelli@irb.usi.ch
http://dx.doi.org/10.1016/j.celrep.2016.04.044

SUMMARY

Dioxygenases of the TET family impact genome functions by converting 5-methylcytosine (5mC) in DNA to 5-hydroxymethylcytosine (5hmC). Here, we identified TET2 as a crucial regulator of mast cell differentiation and proliferation. In the absence of TET2, mast cells showed disrupted gene expression and altered genome-wide 5hmC deposition, especially at enhancers and in the proximity of downregulated genes. Impaired differentiation of *Tet2*-ablated cells could be relieved or further exacerbated by modulating the activity of other TET family members, and mechanistically it could be linked to the dysregulated expression of C/EBP family transcription factors. Conversely, the marked increase in proliferation induced by the loss of TET2 could be rescued exclusively by re-expression of wild-type or catalytically inactive TET2. Our data indicate that, in the absence of TET2, mast cell differentiation is under the control of compensatory mechanisms mediated by other TET family members, while proliferation is strictly dependent on TET2 expression.

INTRODUCTION

DNA methylation at promoters is traditionally considered a stable modification linked to gene silencing and with pivotal regulatory roles in mammalian development. The Ten-Eleven-Translocation (TET) 1–3 proteins are α-ketoglutarate and Fe^{2+}-dependent enzymes able to epigenetically alter DNA by oxidizing 5-methylcytosine (5mC) to 5-hydroxymethylcytosine (5hmC) and further oxidation products (Ito et al., 2011; Tahiliani et al., 2009). Oxidized cytosines serve as intermediates in the process of DNA demethylation, enabling the dynamic turnover of this modification. Moreover, due to the existence of 5mC- and 5hmC-selective or preferential binders, including a broad panel of adapters and chromatin regulators (Pastor et al., 2013), TET activity also directly controls the recruitment of proteins or complexes to methylated DNA.

Different TET family members can have unique and non-overlapping functions, as highlighted by the phenotypes displayed by TET-deficient animals. While the phenotype of mice lacking TET1 is quite mild, mice lacking TET2 display late-onset hematological abnormalities and lack of TET3 is embryonic lethal (reviewed in Pastor et al., 2013). In hematopoietic stem cells (HSCs), lack of TET2 leads to decreased global genomic levels of 5hmC, increased size of the progenitor pool, and enhanced multi-lineage repopulating ability, with a developmental skewing toward the monocyte/macrophage lineage (An et al., 2015; Ko et al., 2011, 2015). A division of labor between the different TET family members in controlling 5hmC distribution is suggested by the observation that, in mouse embryonic stem cells (mESCs), TET1 is primarily responsible for 5hmC modifications at the level of promoter regions and transcriptional start sites (TSSs), whereas TET2 mostly regulates levels of 5hmC at enhancers and in gene bodies (Hon et al., 2014; Huang et al., 2014; Williams et al., 2011). In addition, TET proteins can play unique roles partly due to their specific interactions with co-regulators, allowing them to modulate gene expression independently of DNA hydroxymethylation. For example, TET2 and TET3 interact with the enzyme *O*-linked β-*N*-acetylglucosamine (O-GlcNAc) transferase (OGT) to facilitate its activity (Chen et al., 2013; Deplus et al., 2013), and TET2 was shown to interact with HDAC2, thus modulating transcription of the *Il6* gene (Zhang et al., 2015). TET2 also can also contribute to gene silencing by facilitating the recruitment of the Polycomb Repressive Complex 2 to CpG dinucleotide-rich gene promoters (Wu et al., 2011). Conversely, TET1 (but not TET2) can be incorporated into the SIN3A co-repressor complex, resulting in transcriptional effects independent of 5hmC (Williams et al., 2011).

As an important link of these protein activities to disease, *TET2* frequently acquires loss-of-function mutations in different types of cancers, notably myeloid neoplasms (Ko et al., 2010), while *TET1* and *TET3* are rarely mutated in hematological malignancies (Abdel-Wahab et al., 2009; Huang and Rao, 2014). In

humans, TET2 also was shown to be involved in neoplastic diseases of mast cells, a cell type belonging to the innate myeloid lineage. Mast cellactivation is involved in the response to a variety of pathogens and allergens, making these cells an important effector type not only in innate immunity but also in allergic reactions and asthma. In addition, alterations in the number, localization, and reactivity of mast cells are typical features of systemic mastocytosis (SM), a myeloproliferative disorder characterized by an increase in mast cell burden (Theoharides et al., 2015). Multiple genetic and epigenetic mechanisms can contribute to the onset and severity of all types of mast cell-related diseases; in SM, overall reduced levels of 5hmC correlated with the burden of the mutated D816V *KIT* oncogene (Leoni et al., 2015), and loss of *TET2* cooperated with the *KIT* D816V mutation to transform mast cells to a more aggressive phenotype (De Vita et al., 2014; Soucie et al., 2012). Although mast cells are central in allergic and anaphylactic reactions and represent the pathogenic cell type in SM, the mechanisms underlying the complexity of mast cell phenotypes upon alteration of levels of genomic 5hmC are unknown.

Here we investigated the role of TET2 in regulating differentiation and functions of mast cells. We found that the lack of TET2 led to a complex phenotype characterized by cell-intrinsic delay in differentiation, defects in cytokine production, as well as pronounced hyperproliferation. These alterations were accompanied by extensive transcriptome changes and altered genome-wide 5hmC distribution, especially at the level of enhancers and in the proximity of (and within) genes that resulted to be downregulated in the absence of *Tet2*. *Tet2* ablation also led to dysregulated expression of several transcription factors (TFs), two of which (C/EBPα and C/EBPε) were validated as contributing to the differentiation defects. Importantly, while the defects in cell differentiation could be further exacerbated or diminished by modulating the activity of other TET family members, the increased proliferation could be normalized only by the re-expression of TET2 regardless of its enzymatic activity. These findings indicate not only compensatory roles of the different TET family members on specific pathways, but also the existence of phenotypes that are strictly TET2 dependent. Overall, our data dissect the role of TET2-mediated regulation of mast cell differentiation and function, uncover transcriptional pathways that are predominantly dysregulated as a consequence of TET2 loss, and identify both enzymatic activity-dependent and -independent functions of TET2 in mast cells.

RESULTS

Altered Differentiation, Proliferation, and Cytokine Expression in the Absence of TET2

To investigate the role of TET2 in mast cell biology, we first assessed the effects of *Tet2* gene deletion on cell differentiation and function. We differentiated mast cells by culturing bone marrow progenitors of *Tet2*-deleted animals (Ko et al., 2011) and wild-type (WT) littermates with IL-3. Cell differentiation was monitored by surface staining of relevant mast cell and myeloid markers (Figure 1A). In these culture conditions, more than 90% of WT ($Tet2^{+/+}$) cells differentiated to mast cells (Kit^+ $Fc\varepsilon RI\alpha^+$) by the end of the third week of culture (Figures 1A–1C) (Deho' et al., 2014; Mayoral et al., 2011; Mayoral and Monticelli, 2010; Rusca et al., 2012); however, $Tet2^{-/-}$ cultures showed reduced percentages of mast cells, as well as aberrant expression of markers for other myeloid cells (Mac1 and Ly6G) (Figure 1A), suggesting delayed or altered differentiation. Cultures from heterozygous littermates showed an intermediate phenotype, pointing toward a gene-dosage effect of *Tet2* expression. Visual inspection of cell morphology was consistent with a differentiation defect (Figure S1A). Complete mast cell differentiation could not be achieved even after 6 weeks of culture (Figure 1B). While after 3 weeks $Tet2^{+/+}$ cultures consisted of $\geq$90% mast cells, only ~50% of the cells in $Tet2^{-/-}$ cultures had reached terminal differentiation (Figure 1C). However, once differentiated, $Tet2^{-/-}$ cells expressed similar levels of Kit and FcεRIα as $Tet^{+/+}$ cells and stably maintained their phenotype over time (Figure S1B). Differentiation performed in the presence of both IL-3 and SCF (another mast cell differentiation and survival factor) did not rescue the differentiation defect associated with *Tet2* deficiency (Figure S1C).

In HSCs, lack of *Tet2* was shown to lead to a cell-autonomous increase in the size of the progenitor pool, delayed differentiation, and skewed development toward the monocyte/macrophage lineage, at least in vitro (Ko et al., 2011). To assess whether the observed defects were due to a cell-intrinsic delayed differentiation to mast cells or to increased differentiation to other myeloid lineages, we evaluated the phenotypic stability of the various subpopulations present in $Tet2^{-/-}$ cultures. $Tet2^{+/+}$ and $Tet2^{-/-}$ cells were differentiated for 10 days and then sorted into $Kit^{-/lo}$ $Fc\varepsilon RI\alpha^-$ progenitors, Kit^- $Fc\varepsilon RI\alpha^+$ intermediates, representing a well-defined granulocyte-monocyte progenitor (GMP) stage (Qi et al., 2013), and Kit^+ $Fc\varepsilon RI\alpha^+$ mast cells; we then followed their fate for up to 24 days. We found that $Tet2^{-/-}$ cells maintained the ability to differentiate from precursors to mast cells through the intermediate GMP stage (Figures S1D and S1E), indicating delayed differentiation in the absence of TET2. We therefore assessed proliferation and effector functions of differentiated mast cells, which were separated as Kit^+ $Fc\varepsilon RI\alpha^+$ in all experiments. First, we evaluated cell survival in response to withdrawal of IL-3, which was unaffected by *Tet2* deletion (Figure S2A). Conversely, by assessing BrdU incorporation in response to IL-3 treatment (Figure S2B) (Deho' et al., 2014), we found that $Tet2^{-/-}$ mast cells showed significant hyperproliferation compared to their $Tet2^{+/+}$ counterparts, while $Tet2^{+/-}$ cells displayed an intermediate phenotype, pointing again toward a gene-dosage effect of *Tet2* in regulating mast cellproliferation (Figures 1D and 1E).

We next assessed cytokine expression. Cells were stimulated with IgE and antigen, followed by intracellular staining for three cytokines that are abundantly produced by activated mast cells, namely IL-6, TNF-α, and IL-13. We observed no difference in basal cytokine expression between $Tet2^{-/-}$ and $Tet2^{+/+}$ cells (Figures S2C–S2E). Upon stimulation, the percentage of cells expressing these cytokines was reduced in $Tet2^{-/-}$ mast cells compared to their WT counterparts, as assessed by intracellular staining (Figures 1F and 1G; Figures S2C and S2D), although the overall amount of secreted cytokines was more comparable, at least after 12 hr of stimulation (Figure S2E). Interestingly, the

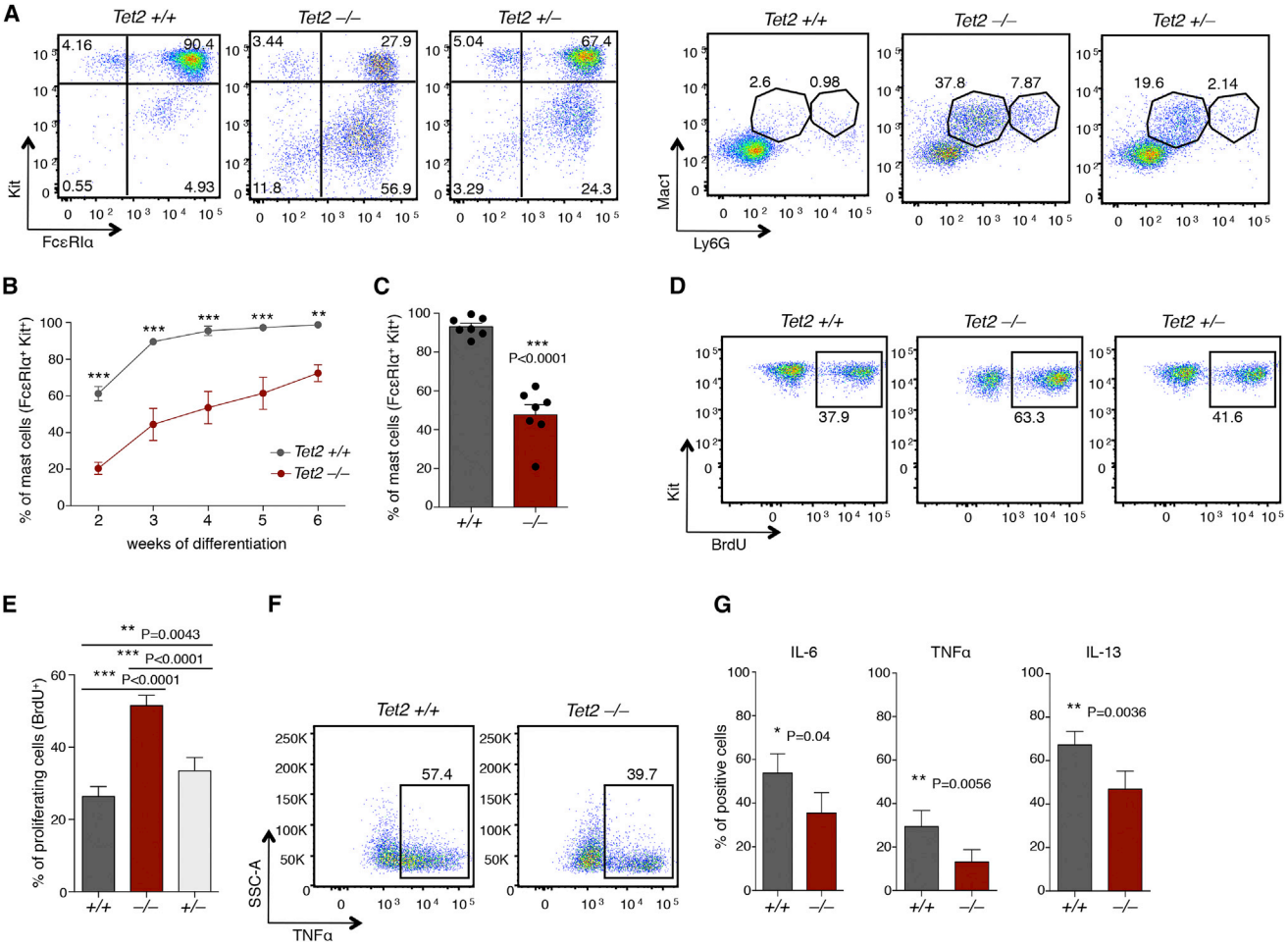

Figure 1. Altered Mast Cell Differentiation, Proliferation, and Effector Functions in the Absence of *Tet2*

(A) Bone marrow cells from $Tet2^{+/+}$, $Tet2^{-/-}$, and $Tet2^{+/-}$ mice were differentiated to mast cells. Shown is one representative surface staining for mast cell markers (Kit and FcεRIα) and other myeloid markers (Mac1 and Ly6G) after 3 weeks of differentiation.

(B) Percentage of Kit^+ $FcεRIα^+$ mast cells in bone marrow cultures of $Tet2^{+/+}$ and $Tet2^{-/-}$ littermates, over 6 weeks of differentiation, is shown (n = 4; two-way ANOVA, ***p < 0.0003 and **p = 0.0084).

(C) Same as (B), except that quantification for seven independent experiments at the third week of differentiation is shown. Each dot represents one biological sample (unpaired t test, two-tailed; mean ± SEM).

(D) Mast cell proliferation was assessed by BrdU incorporation assay. Kit^+ $FcεRIα^+$ mast cells were either physically separated at least 1 day before the experiment or were gated at the analysis step.

(E) Same as (D), except that the compiled result of 13 independent experiments is shown (paired t test, two tailed; mean ± SEM).

(F) Cells were stimulated with IgE and antigen before intracellular cytokine staining. One representative staining for TNF-α expression is shown.

(G) Same as (F), except that the compiled results for six (IL-6 and TNF-α) or seven (IL-13) independent experiments are shown (paired t test, two tailed; mean ± SEM).

See also Figures S1 and S2.

ability of $Tet2^{-/-}$ mast cells to release the pre-stored content of cytoplasmic granules was comparable to that of their WT counterparts (Figure S2F), suggesting that some effector functions of differentiated cells were unaffected by *Tet2* deficiency. Overall, these data point toward a key role of TET2 in regulating predominantly mast cell differentiation and proliferation.

Transcriptional Impact of *Tet2* Deletion in Mast Cells

To investigate the altered gene expression programs underlying the phenotypic defects of $Tet2^{-/-}$ mast cells, we performed RNA sequencing (RNA-seq) to compare the transcriptome of these cells with that of WT mast cells. To compare populations that were as homogenous as possible, we sorted $Tet2^{-/-}$ mast cells (Kit^+ $FcεRIα^+$) to ≥95% purity. We profiled two independent biological replicates using >80 million mapped paired-end reads per sample. Differentially expressed genes (DEGs) were identified using Cuffdiff (Trapnell et al., 2013) with standard parameters (fold change ≥ 2, p ≤ 0.05, and fragments per kilobase of exon per million fragments mapped [FPKM] > 1 in at least one of the two conditions). Pairwise analysis of the transcriptomes

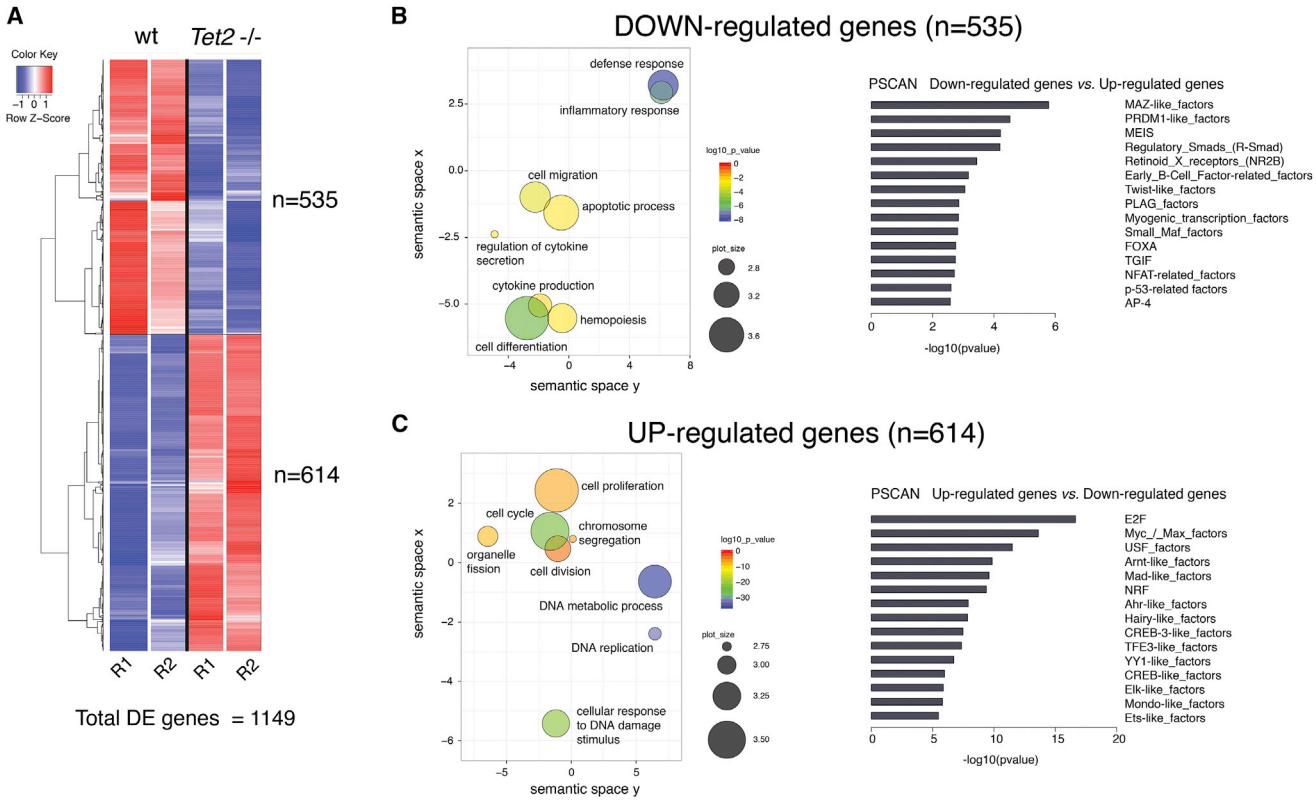

Figure 2. RNA-Seq Analysis Identifies Dysregulated Genes and Functional Pathways in *Tet2*$^{-/-}$ Mast Cells

(A) Total RNA from *Tet2*$^{+/+}$ and *Tet2*$^{-/-}$ mast cells was used for RNA-seq. DEGs are shown in a hierarchically clustered heatmap. For hierarchical clustering, distance metric between rows was calculated according to the Pearson correlation on the log2 of FPKM values and then normalized by *Z* score. Lowest *Z* score values are dark blue and highest values are bright red.

(B and C) Enriched GO functional categories (left) and over-represented TF consensus DNA-binding sites (right) in up- (C) and downregulated (B) genes were identified using REVIGO and PSCAN, respectively. GO terms are visualized in semantic similarity-based scatterplots. Bubble color indicates the p value as follows: blue and green bubbles are GO terms with more significant p values compared to orange and red bubbles. Bubble size shows how much the GO term is represented in the GO database. Selected representative categories are shown. For PSCAN analyses, each over-represented TF subfamily is shown according to the obtained Welch p values (−log10).

See also Figure S3.

of WT and *Tet2*$^{-/-}$ mast cells identified 1,149 DEGs that were either downregulated (n = 535) or upregulated (n = 614) in *Tet2*$^{-/-}$ cells (Figure 2A), pointing toward complex (and likely both direct and indirect) effects of TET2 on the mast cell transcriptome (Lu et al., 2014). A gene ontology (GO) analysis of the DEGs is shown in Figures 2B and 2C. GO categories with highly significant p values for the downregulated genes included inflammatory and defense responses, as well as cytokine production and cell differentiation, all consistent with the observed dysregulated mast cell functions (Figure 2B). In keeping with the hyperproliferative phenotype of *Tet2*$^{-/-}$ mast cells, the top-ranking GO categories for the upregulated genes included cell division-related terms, such as cell cycle and proliferation, DNA replication and metabolic processes, and DNA damage and repair responses (Figure 2C).

To identify possible TFs that could be common regulators of the genes affected by *Tet2* deletion, we analyzed the regions surrounding the TSSs (from −500 bp to +250 bp) of the identified DEGs utilizing PSCAN, a computational tool that investigates over- or under-represented TF consensus DNA-binding motifs (position weigh matrixes [PWMs], Zambelli et al., 2009). Consistent with the observed phenotype and the enriched GO categories, PSCAN analysis of PWMs at upregulated genes revealed an enrichment in consensus DNA-binding motifs recognized by TF families controlling cell cycle and proliferation, such as E2Fs and Myc/Max (Figure 2C) (Amati et al., 2001; Gallant and Steiger, 2009; Ren et al., 2002). The p values of the PWMs retrieved by the same analysis at downregulated genes (including MAZ-like TFs, MEIS, and others) were less significant, which may be in line with the possibility that, rather than affecting the function of specific TFs, TET2 loss impacts a broad and heterogeneous set of genomic regions and regulatory elements.

We validated our RNA-seq data using at least four independent samples of *Tet2*$^{+/+}$ and *Tet2*$^{-/-}$ mast cells by analyzing the mRNA levels of selected DEGs, such as the genes encoding for the myeloperoxidase *Mpo*, the TF C/EBPα, the mast cell protease 8 (*Mcpt8*), the serine protease *Prss34*, the adhesion

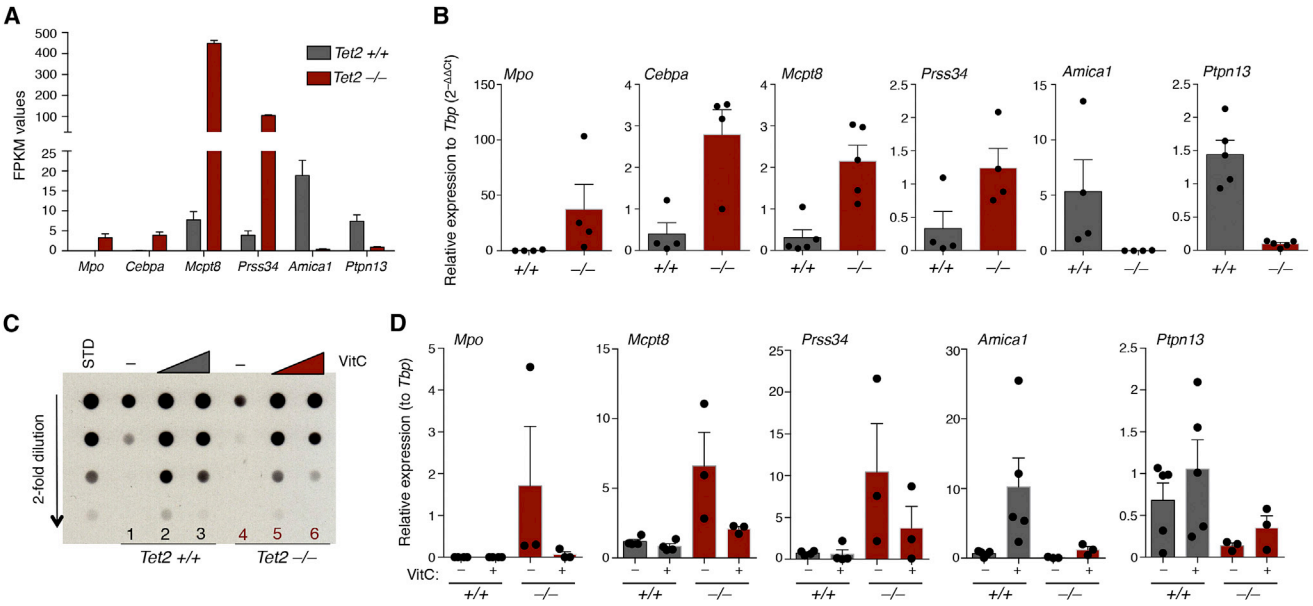

Figure 3. VitC Treatment Restores Gene Expression in *Tet2*$^{-/-}$ Mast Cells

(A) FPKM values are plotted for selected DEGs identified by RNA-seq (mean ± SEM).

(B) The same genes as in (A) were validated by qRT-PCR. Each dot represents one independent biological sample (n = at least 4). Shown is the expression relative to the endogenous control *Tbp* and to one *Tet2*$^{+/+}$ sample.

(C) After 2.5 weeks of differentiation, *Tet2*$^{+/+}$ and *Tet2*$^{-/-}$ mast cells were either left untreated or were supplemented with 10 and 50 μg/ml VitC for 10 days. The DNA was extracted and 2-fold dilutions starting from 500 ng were spotted on a membrane. The 5hmC content was assessed using an anti-5hmC antibody.

(D) Cells were treated as in (C) with medium supplemented with 50 μg/ml VitC for 10 days. Total RNA was then extracted and gene expression analyzed by qRT-PCR. Shown is the expression relative to *Tbp*. Expression of all genes also is related to one *Tet2*$^{+/+}$ sample except for *Mpo* that was mostly undetectable in *Tet2*$^{+/+}$ cells (n = at least 3, mean ± SEM).

See also Figure S4.

molecule *Amica1*, and the tyrosine phosphatase *Ptpn13* (Figures 3A and 3B). We also assessed microRNA (miRNA) expression globally by array profiling. We did not detect any significant and reproducible change in miRNA expression (Figure S3), suggesting that miRNA expression in mast cells is not significantly influenced by the lack of TET2 and is therefore unlikely to explain the phenotypes observed in the absence of this enzyme.

TET3 Can Only Partially Compensate for the Lack of TET2 in Mast Cells

To investigate whether the alterations in gene expression that were observed in the absence of TET2 could be rescued by the enzymatic activity of other TET family members (namely TET1 and TET3), we took advantage of the fact that vitamin C (VitC) enhances the catalytic activity of TET proteins by acting as a co-factor that maintains the essential atom of iron in the catalytic site in a reduced state (Fe^{2+}) (Blaschke et al., 2013; Yin et al., 2013). Differentiated mast cells were treated with VitC prior to analysis of overall levels of genomic 5hmC by dot blot (Figure 3C). *Tet2*$^{-/-}$ mast cells had reduced levels of 5hmC compared to their WT counterparts (compare lanes 1 and 4); medium supplementation with VitC, however, strongly increased the global 5hmC levels in both *Tet2*$^{+/+}$ and *Tet2*$^{-/-}$ mast cells (Figure 3C). In the absence of TET2, such effect was most likely due to the enhanced enzymatic activity of other TET family members (Yue et al., 2016), since VitC treatment did not significantly increase the expression of any *Tet* mRNA (Figure S4).

We next assessed whether enhanced 5hmC deposition driven by VitC supplementation could rescue the differential expression of TET2-regulated genes. VitC treatment induced a partial normalization of gene expression, since genes overexpressed in *Tet2*$^{-/-}$ cells (*Mpo*, *Mcpt8*, and *Prss34*) returned to near-normal levels. The expression of some downregulated genes (*Amica1* and *Ptpn13*) was induced, albeit modestly (Figure 3D). Our data indicate that altered gene expression in the absence of *Tet2* is mainly due to reduced 5hmC production, and this can be rescued, at least in part, by enhancing the activity of other TET family members.

Since we observed that enhanced 5hmC deposition could partially rescue gene expression changes due to the absence of *Tet2*, we assessed whether it also could rescue mast cell proliferation, effector functions, and differentiation. First, we assessed cell proliferation in *Tet2*$^{-/-}$ mast cells treated with or without VitC. Strikingly, the difference in proliferation between *Tet2*$^{-/-}$ and *Tet2*$^{+/+}$ cells remained unaffected by VitC treatment (Figures 4A and 4B), suggesting that the hyperproliferation induced by the absence of *Tet2* was strictly TET2 dependent and independent of the enzymatic activity of other TET proteins. Conversely, VitC treatment was sufficient to fully restore the ability of cells to express IL-6, TNF-α, and IL-13 at levels that were

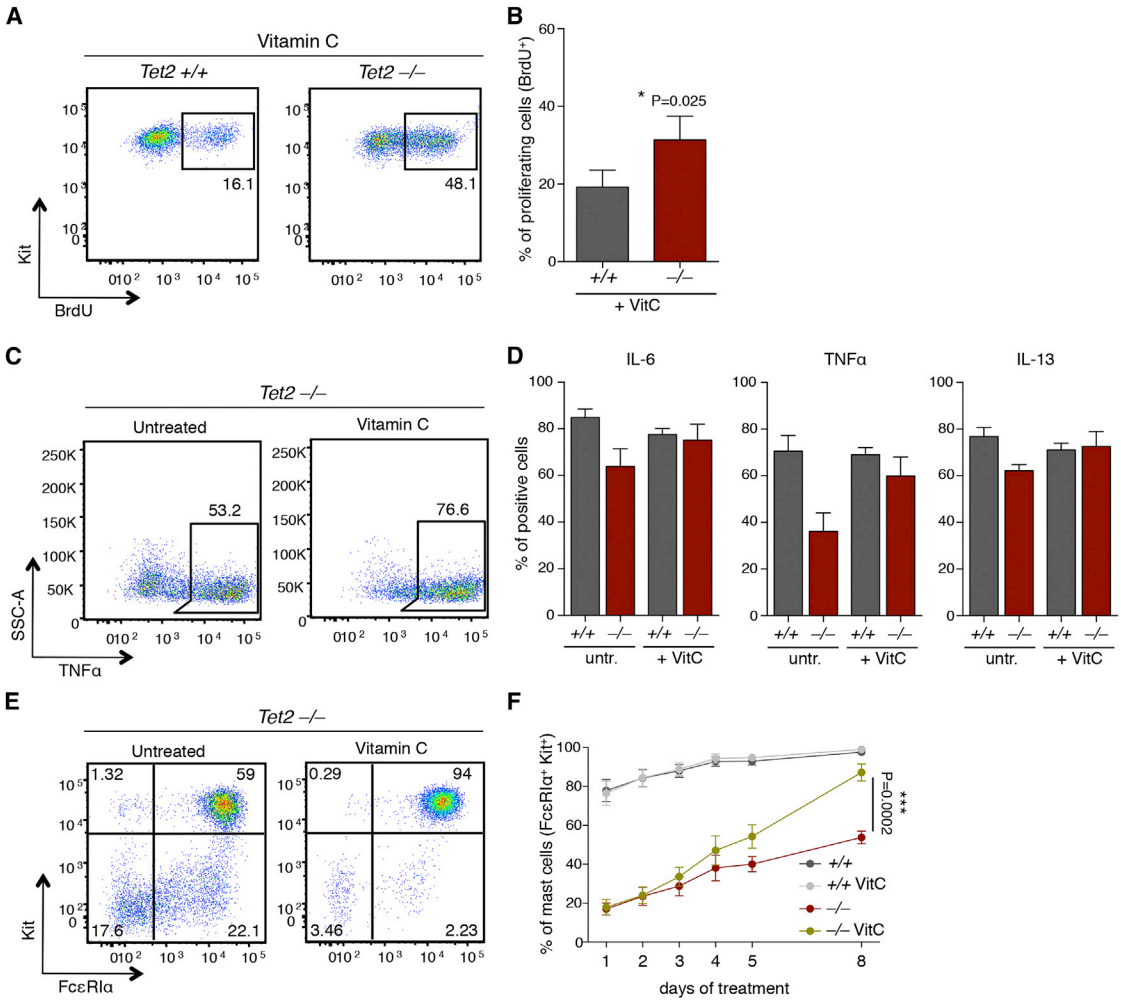

Figure 4. VitC Treatment Restores Mast Cell Differentiation and Cytokine Production, but Does Not Normalize Proliferation

(A) *Tet2*$^{+/+}$ and *Tet2*$^{-/-}$ mast cells were treated with 50 μg/ml VitC for 10 days, after which proliferation was assessed by BrdU incorporation. One representative experiment is shown.

(B) Same as (A), except that the results of seven experiments are shown (paired t test, two tailed; mean ± SEM).

(C) *Tet2*$^{-/-}$ mast cells were treated as in (A) prior to intracellular cytokine staining. One representative experiment for TNF-α is shown.

(D) Same as (C), except that the results of five (IL-6 and TNF-α) or three (IL-13) experiments are shown.

(E) *Tet2*$^{+/+}$ and *Tet2*$^{-/-}$ bone marrow cells were differentiated to mast cells for 2 weeks, after which culture medium was further supplemented with 50 μg/ml VitC for 8 days. The percentage of mast cells in culture was assessed by surface staining for Kit and FcεRIα. One representative experiment is shown.

(F) Same as (E), except that the results of four experiments are shown. Statistical analysis was performed with two-way ANOVA.

comparable to those of WT cells (Figures 4C and 4D). VitC treatment was similarly able to fully complement the absence of TET2 by completely rescuing mast cell differentiation (Figures 4E and 4F).

To further investigate whether modulation of the expression of other TET proteins could influence mast cell functions, we depleted TET3 in *Tet2*$^{-/-}$ mast cells using small hairpin RNAs (shRNAs). To test the efficacy of the shRNA sequences, we first transduced a neuronal cell line (Cashman et al., 1992), as neurons express high levels of TET3 (Hahn et al., 2013), and we assessed global 5hmC levels 7 days after transduction (Figure 5A). We observed an ~30% reduction in levels of *Tet3* mRNA in these cells, which corresponded to a detectable reduction (up to ~24%) in the global level of 5hmC (Figure 5A). We therefore used lentiviral transduction of TET3-specific shRNAs in differentiated *Tet2*$^{-/-}$ mast cells, achieving up to a 43% reduction in *Tet3* expression (Figure 5B). Concordant with the fact that VitC could not rescue mast cell hyperproliferation in the absence of *Tet2*, reduction of TET3 expression had no effect on mast cell-proliferation in *Tet2*$^{-/-}$ cells (Figures 5C and 5D). Conversely, depletion of TET3 in *Tet2*$^{-/-}$ bone marrow precursors exacerbated the phenotype observed in the absence of *Tet2* and led to a further delay in mast cell differentiation (Figures 5E and 5F). Our data indicate that, while cytokine production and mast cell differentiation could be fully restored by mechanisms that modulate expression or activity of other TET proteins,

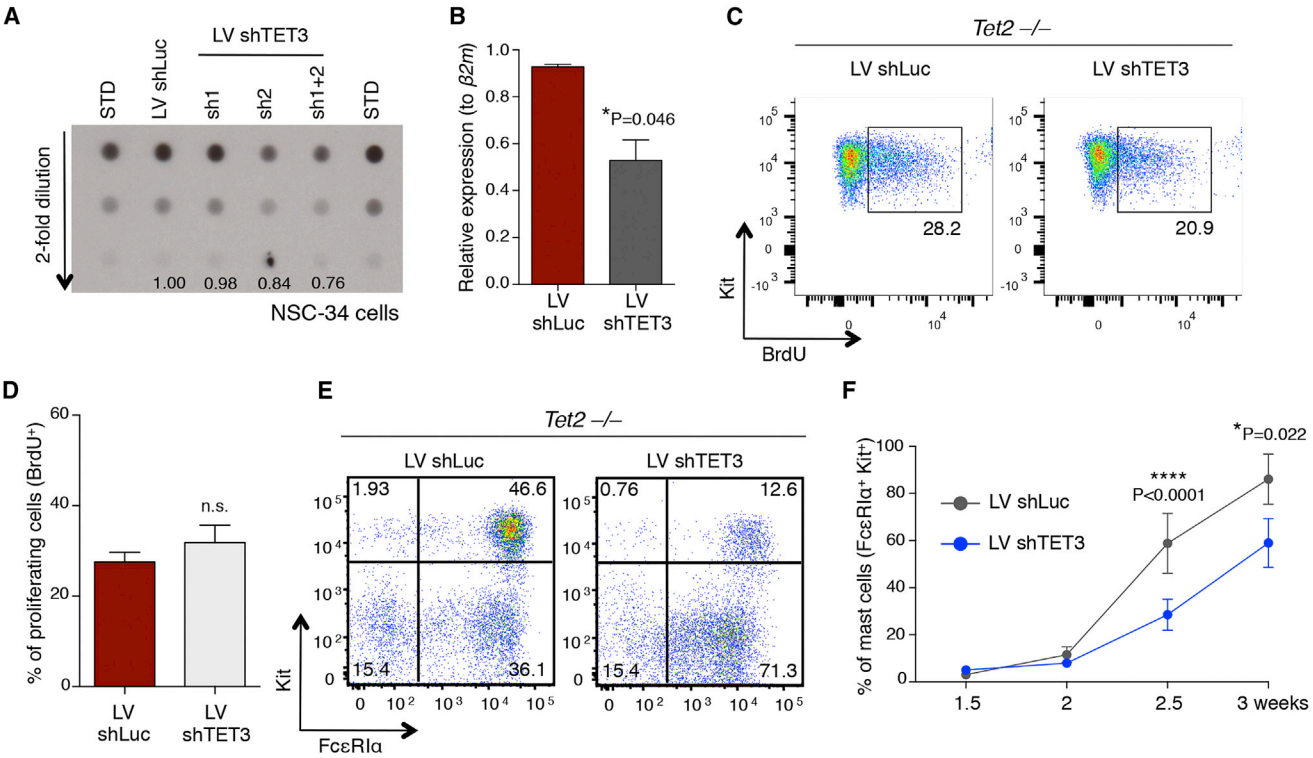

Figure 5. Knockdown of TET3 Further Exacerbates the Differentiation Defect of *Tet2*$^{-/-}$ Cells, but Does Not Affect Proliferation

(A) NSC-34 cells were transduced with lentiviruses expressing either an irrelevant control hairpin (shLuc) or two different shRNAs against murine TET3 (sh1 and sh2), alone or in combination. Levels of genomic 5hmC were measured by dot blot. The 2-fold dilution of DNA, starting from 100 ng, was spotted on the membrane. Values of relative quantification are indicated on the blot.

(B) *Tet2*$^{-/-}$ bone marrow cells were transduced with a mixture of shRNAs against TET3 as in (A) and the expression of *Tet3* mRNA was measured by qRT-PCR. Shown is the result of two independent experiments each performed with two biological replicates. Data were normalized to the expression of β2 microglobulin (unpaired t test, two tailed; mean ± SEM).

(C) Same as (B), except that proliferation of *Tet2*$^{-/-}$ cells transduced with a control hairpin or shTet3 was measured by BrdU incorporation assay. One representative result is shown.

(D) Same as (C), except that the results of five experiments are shown (paired t test, two tailed; mean ± SEM).

(E) *Tet2*$^{-/-}$ bone marrow precursors were transduced as in (B), and cell differentiation was followed over time by surface staining for Kit and FcεRIα. Shown is one representative result after 2.5 weeks of differentiation.

(F) Same as (E), except that the data of two different experiments are shown, each performed with two independent biological replicates. Statistical analysis was performed with two-way ANOVA.

control of mast cell proliferation appeared to be predominantly TET2 dependent.

Altered Expression of C/EBP TFs Is Sufficient to Impair Mast Cell Differentiation

Since one of the major phenotypes observed in *Tet2*$^{-/-}$ cells was a delay in their differentiation, which could most likely also contribute to their reduced cytokine production (Tsai et al., 1991), we investigated whether dysregulated expression of TFs involved in myeloid differentiation could explain such a phenotype. We found that *Cebpa* and *Cebpe* were both upregulated in *Tet2*$^{-/-}$ cells (Figures 3A and 6A, left panel). Because C/EBPε is involved in regulating multiple steps of myeloid differentiation, especially toward granulocytic lineages (Paul et al., 2015; Yamanaka et al., 1997), and C/EBPα was shown to influence the choice in the differentiation toward mast cells or granulocytes (Iwasaki et al., 2006; Qi et al., 2013), we investigated whether dysregulated expression of these TFs could contribute to the differentiation delay observed in the absence of *Tet2*. We transduced hematopoietic precursors with vectors to express either C/EBPε (Figures 6A–6D) or C/EBPα (Figures 6E and 6F). Expression of C/EBP TFs in *Tet2*$^{+/+}$ cells led to reduced and delayed mast cell differentiation (Figures 6B and 6F), resembling the phenotype observed in the absence of *Tet2*, which could therefore be explained, at least in part, by the dysregulated expression of C/EBP family members. Accordingly, forced expression of *Cebpe* in *Tet2*$^{-/-}$ mast cells (thereby further increasing its already high expression) led to an even greater inability of the cells to differentiate (Figure 6D). In agreement with the effect of C/EBP TFs on differentiation, we also found that overexpression of C/EBPε induced expression of at least some of the genes that were found to be induced in the absence of *Tet2*, namely *Mcpt8* and *Prss34* (Figure 6C). Our data show that increased expression of either *Cebpa* or *Cebpe* is sufficient

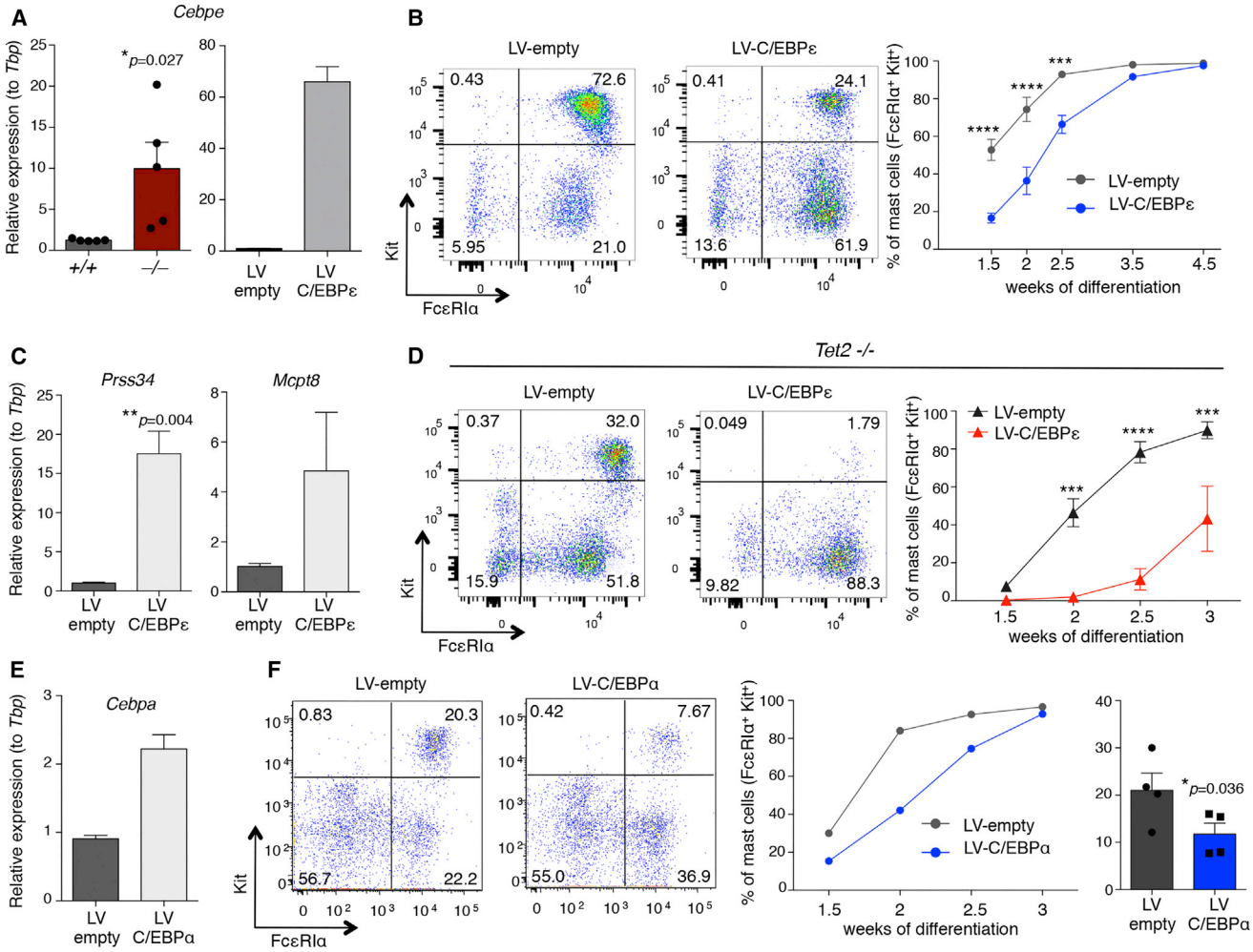

Figure 6. Dysregulated Expression of C/EBP TFs Leads to Delayed Mast Cell Differentiation

(A) (Left) Expression of *Cebpe* was assessed in *Tet2*$^{+/+}$ and *Tet2*$^{-/-}$ mast cells by qRT-PCR (n = 5, each dot represents one biological sample; unpaired t test, two tailed; mean ± SEM). (Right) *Tet2*$^{+/+}$ Lin^{-} bone marrow hematopoietic precursors were transduced with a lentiviral vector to express C/EBPε. Expression of *Cebpe* was assessed by qRT-PCR. Endogenous control: *Tbp*.

(B) *Tet2*$^{+/+}$ Lin^{-} hematopoietic precursors were transduced as in (A), and mast cell differentiation was assessed over time by surface staining for Kit and FcεRIα. One representative staining after 2 weeks of differentiation is shown on the left, while the graph on the right shows the results of four independent transductions (two-way ANOVA, ****p < 0.0001 and ***p = 0.0001).

(C) Same as (B), except that the expression of selected mast cell proteases was measured by qRT-PCR (n = 4, mean ± SEM).

(D) Same as (A) and (B), except that forced expression of C/EBP was performed on bone marrow cells of *Tet2*$^{-/-}$ mice. One representative staining at 2 weeks of differentiation is shown on the left; the graph on the right shows the results of six transductions (two-way ANOVA, pvalues are, from left to right, ***p = 0.0005, ****p < 0.0001, and ***p = 0.0002).

(E) *Tet2*$^{+/+}$ Lin^{-} hematopoietic precursors were transduced to express C/EBPα or a control vector. Expression of *Cebpa* was assessed by qRT-PCR.

(F) Same as (E), with mast cell differentiation assessed by surface staining for Kit and FcεRIα. One representative staining after 1.5 weeks of differentiation is shown on the left; the graph in the middle shows one representative experiment over time, while the bar graph on the right shows the results of three different experiments after 1.5 weeks (paired t test, two tailed; mean ± SEM).

to determine defective mast cell differentiation, resembling the phenotype observed in *Tet2*$^{-/-}$ cells.

Altered Genome-wide 5hmC Deposition in the Absence of *Tet2*

To gain further insights on the molecular mechanisms that regulate mast cell functions in the absence of TET2, we investigated changes in genome-wide 5hmC deposition by glucosylation, periodate oxidation, and biotinylation (GLIB)-based enrichment of 5hmC and sequencing (GLIB-seq). First, *Tet2*$^{-/-}$ cells showed an overall enrichment of regions depleted of 5hmC compared to regions where this modification was increased (Figure 7A; Figure S5). Specifically, 2,715 peaks were hypo-hydroxymethylated in *Tet2*$^{-/-}$ cells, of which 2,588 classified as distal and 127 as proximal relative to the TSSs of annotated genes. In comparison, only 468 peaks resulted in hyper-hydroxymethylated (437

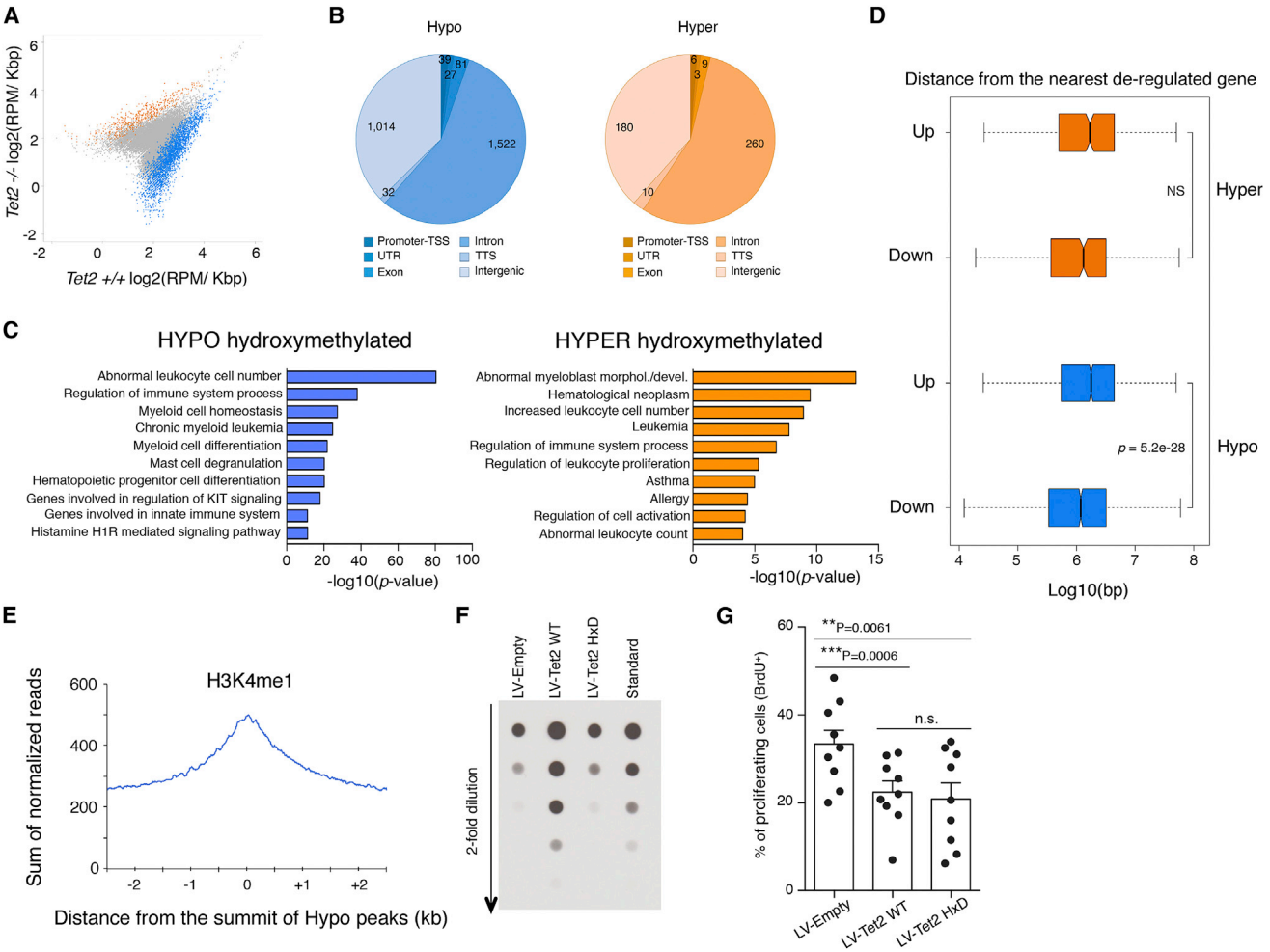

Figure 7. TET2 Reconstitution Reduces Mast Cell Proliferation, Independently of 5hmC Modification

(A) Differentially hydroxymethylated distal regions in *Tet2*$^{-/-}$ mast cells. Hyper-hydroxymethylated peaks are depicted in red, hypo-hydroxymethylated in blue, and unchanged peaks in gray.

(B) Genomic location of the differentially hydroxymethylated regions is shown.

(C) Functional enrichment analysis of differentially hydroxymethylated regions was performed using GREAT. Selected categories are shown; see Table S8 for the full list of significant categories.

(D) Distance of hyper- and hypo-hydroxymethylated regions from the nearest dysregulated (up- or downregulated) gene is shown.

(E) Distance of H3K4me1 peaks, as assessed by ChIP-seq of *Tet2*$^{+/+}$ cells, from the summit of hypo-hydroxymethylated regions is shown.

(F) *Tet2*$^{-/-}$ mast cells were transduced with an empty vector or with vectors expressing WT or catalytically inactive TET2 (HxD). Levels of 5hmC were measured by dot blot. One representative experiment is shown.

(G) Proliferation of mast cells transduced as in (F) was assessed by BrdU incorporation assay. Each dot represents one independent experiment (paired t test, two tailed; mean ± SEM).

See also Figure S5.

distal and 31 proximal). Finally, 9,725 peaks (9,022 distal and 703 proximal) were common and did not change, while 11,011 peaks could not be consistently classified. An analysis of the relative distribution of the genomic location of the hypo- and hyper-hydroxymethylated peaks revealed that the vast majority of differentially hydroxymethylated peaks was localized in introns and intergenic regions (Figure 7B).

Interestingly, a GREAT analysis (McLean et al., 2010) of the differentially hydroxymethylated regions identified categories relevant to leukocyte differentiation and proliferation, malignant transformation, and mast cell-related processes such as KIT and histamine signaling (Figure 7C). To better understand the correlation between altered hydroxymethylation and altered gene expression in *Tet2*$^{-/-}$ cells, we evaluated the distance of the hypo- and hyper-hydroxymethylated regions from genes that were up- or downregulated based on RNA-seq data. While the hyper-hydroxymethylated peaks did not show any significant difference in their distance from either up- or downregulated genes, the hypo-hydroxymethyated peaks were significantly closer to genes that were downregulated in

Tet2$^{-/-}$ cells (Figure 7D), suggesting that, at least for a subset of genes, levels of TET2-dependent 5hmC may be important to maintain proper levels of expression.

To better characterize the functional relevance of such hypo-hydroxymethylated regions in gene expression, we assessed the genome-wide distribution of H3K4me1 (monomethylated lysine 4 on the histone H3 N-terminal tail) by chromatin immunoprecipitation and sequencing (ChIP-seq), since this is a modification known to mark enhancers (Heintzman et al., 2007, 2009). We evaluated the distance of H3K4me1 peaks from the summit of hypo-hydroxymethylated peaks (Figure 7E), and we found that hypo-hydroxymethylated regions in *Tet2*$^{-/-}$ cells tended to overlap with H3K4me1-marked regions, a result consistent with data obtained in other cell types (Hon et al., 2014; Rasmussen et al., 2015). These data indicate that many genomic regions are affected by the lack of *Tet2* in mast cells and that hypo-hydroxymethylated regions are significantly closer to downregulated genes and often associated with transcriptional enhancers, suggesting a direct role for TET2-derived 5hmC in modulating proper expression of these genes, potentially through the maintenance of a demethylated state at the level of enhancers (Rasmussen et al., 2015).

TET2 Reconstitution, Independent of Its Enzymatic Activity, Normalizes Mast Cell Proliferation

As shown above, proliferation of *Tet2*$^{-/-}$ mast cells was not significantly influenced by modulating levels of 5hmC. Therefore, to gain further insights on the molecular mechanisms that could lead to dysregulated proliferation in *Tet2*$^{-/-}$ mast cells, we assessed the role of TET2 enzymatic activity in regulating mast cell proliferation. We reconstituted *Tet2*$^{-/-}$ mast cells with lentiviral vectors expressing the TET2 carboxy-terminal catalytic domain (amino acids 990–1,912 of mouse TET2), with or without substitutions in the H × D motif (H1302Y and D1304A) that ablate its enzymatic activity (Ko et al., 2010). As expected, transfection of HEK293 cells with the WT, but not the mutated plasmid, showed increased levels of 5hmC in the nucleus, as assessed by immunofluorescence (Figure S6A). Despite higher levels of expression of the mutated TET2 H × D compared to TET2 WT (Figure S6B), only TET2 WT was able to increase the levels of overall genomic 5hmC in *Tet2*$^{-/-}$ mast cells (Figure 7F). Analysis of the expression of genes that were dysregulated in the absence of TET2 showed partial recovery upon reconstitution, mostly mediated by TET2 WT (Figure S6C). We subsequently assessed mast cell proliferation by BrdU incorporation. Surprisingly, both WT and H × D TET2 were able to reduce mast cell proliferation to a comparable degree that was significantly lower than that obtained with the control vector (Figure 7G). These data suggest that mast cell proliferation is primarily regulated by an enzymatic activity-independent function of TET2, consistent also with the fact that we could not influence cell proliferation by either VitC treatment or TET3 knockdown (Figures 4A, 4B, 5C, and 5D). These data indicate that TET2 expression, but not its enzymatic activity, is required to restrain mast cell proliferation, most likely through the interaction with other partner proteins.

In summary, our data revealed a complex phenotype induced by the lack of *Tet2* in mast cells, comprising primarily delayed differentiation and significant hyperproliferation. While the differentiation defect could be rescued by mechanisms other than TET2 expression (for example by the enhanced activity of TET1 and TET3) and it was linked to dysregulated expression of C/EBP TFs, the increased proliferation appeared to be predominantly dependent on TET2 and uncoupled from changes in overall 5hmC deposition in mast cells.

DISCUSSION

Our study establishes an important role for TET2 in regulating mast cell differentiation, proliferation, and functions, which may impact all mast cell-related diseases. The absence of *Tet2* led to a widespread alteration of 5hmC distribution and gene expression; specifically, we found that many genomic regions (especially enhancers) showed reduced levels of 5hmC, and they were associated with functional categories related to myeloid cell homeostasis and mast cell activities. Among the genes with altered expression, we found that increased levels of C/EBP TFs could, at least in part, contribute to the delayed differentiation observed in *Tet2*$^{-/-}$ cells. Interestingly, there was no specific single TF that stood out as a potential candidate to modulate cell proliferation, suggesting a more widespread network of modifications leading to cell-cycle dysregulation. Further highlighting the complex role of TET2 in regulating cell proliferation, this process could not be influenced by modulating 5hmC deposition in *Tet2*$^{-/-}$ cells, and could only be rescued by re-expression of TET2 itself, regardless of its catalytic activity.

Although the exact mechanism by which TET2 regulates cell proliferation remains to be understood, it is likely to involve interactions with other co-regulators. For example, incorporation of TET1 into the SIN3A corepressor complex resulted in transcriptional effects independent of the conversion of 5mC to 5hmC (Williams et al., 2011). While TET1 is expressed in mast cells at very low levels, a related mechanism may be at play for TET2-mediated regulation of cell proliferation. Indeed, TET2 is able to recruit HDAC2 during resolution of inflammation in myeloid cells, leading to the repression of *Il6* gene transcription via histone deacetylation, that is, independently of hydroxymethylation (Zhang et al., 2015). Although we tested a small subset of genes, we observed only a very limited ability of the catalytic inactive TET2 to rescue gene expression; this was in agreement with the fact that changes in gene expression in *Tet2*-deleted cells appeared to be predominantly 5hmC dependent. What is the exact proportion of genes depending on TET2 catalytic activity, TET2 protein itself, or both remains to be investigated. Previous reports investigating TET-interacting complexes mapped the main region mediating protein-protein interactions to the carboxy-terminal catalytic domain of TET2 (Chen et al., 2013; Zhang et al., 2015); consistently, we found that this same region was able to rescue proliferation of *Tet2*-deleted mast cells, independently of its catalytic activity. TET2 also was shown to interact with OGT and to promote its enzymatic activity (Chen et al., 2013; Deplus et al., 2013). Although we could not observe any strong change in overall protein O-GlcNAcylation in *Tet2*-deleted mast cells (Figure S6D), more subtle differences cannot be ruled out.

To fully comprehend the complexity of epigenetic modifications, which for the most part cannot be easily recapitulated by

dysregulated activity of one or a few TFs, it is also important to recognize that DNA methylation dynamics can lead not only to altered expression of TFs but also to altered affinity and specificity of TF binding. Indeed, a recent work identified protein readers for 5mC and its oxidized derivatives by utilizing quantitative mass-spectrometry-based proteomics (Spruijt et al., 2013), revealing that each cytosine modification was able to recruit distinct and dynamic sets of proteins, which were only partially overlapping. More specifically for C/EBP TFs, CpG methylation of cAMP response element (CRE) sequences also was shown to enhance binding of C/EBPα compared to the unmethylated form (Rishi et al., 2010). Taken together, changes in DNA methylation can determine both direct alterations in gene transcription and also altered binding of TFs and co-regulators, potentially resulting in complex phenotypes that cannot be easily associated with only one or a few genomic loci. In summary, we found that TET2 regulates various aspects of mast cell biology, most notably cell differentiation and proliferation. While mast cell differentiation could be compensated for by modulating the activity of other TET proteins, mast cell proliferation was strictly dependent on TET2, with no compensatory effects by other TET family members, further indicating that TET2 exerts functions that can be independent from its enzymatic activity.

EXPERIMENTAL PROCEDURES

Mice and Cell Cultures

Mast cells were differentiated from the bone marrow of *Tet2*$^{-/-}$ mice (Ko et al., 2011) and their *Tet2*$^{+/+}$ and *Tet2*$^{+/-}$ littermates in the presence of IL-3 as described (Deho' et al., 2014; Mayoral and Monticelli, 2010). Mice were 8–12 weeks of age and both male and female, although for the majority of the experiments male cells were used. All animal studies were performed in accordance with the Swiss Federal Veterinary Office guidelines and were approved by the Dipartimento della Sanita' e della Socialita'. When needed, in order to enrich *Tet2*$^{-/-}$ mast cells to levels comparable to the *Tet2*$^{+/+}$ cultures, cells were stained for the surface markers Kit and/or FcεRIα and separated by either sorting or positive selection using anti-PE-MicroBeads (Miltenyi Biotec). Alternatively, cells were negatively selected by depleting the Gr1^{+} Mac1^{+} populations. All of these methods resulted in an enrichment of purified mast cells up to at least 89%. VitC was added to cells already differentiated for 2.5 weeks and used at 10–50 μg/ml for 8–10 days. The NSC-34 murine motor neuron-like cell line (Cashman et al., 1992) was maintained in DMEM, supplemented with 5% heat-inactivated fetal bovine serum (FBS), 100 U/ml penicillin, 100 mg/ml streptomycin, and 2mM L-glutamine. HEK293T cells were maintained in DMEM supplemented with 10% FBS, L-glutamine, penicillin, streptomycin, 0.1 mM nonessential amino acids, and 50 mM β-mercaptoethanol.

Surface and Intracellular Cytokine Staining

The following antibodies were used for surface staining (all from BioLegend): CD117 (Kit)-APC/Cy7 (or APC); FcεRIα-PE; Ly6G (Gr1)-PE/Cy7 (or fluorescein isothiocyanate [FITC]); and CD11b (Mac1)-Pacific blue. Intracellular cytokine staining was performed exactly as described (Deho' et al., 2014; Rusca et al., 2012). Briefly, cells were stimulated with 1 μg/ml IgE-anti-DNP and 0.2 μg/ml HSA-DNP (both from Sigma) for 3 hr, with the addition of 10 μg/ml brefeldin A in the last 2 hr of stimulation. Cells were fixed with 4% paraformaldehyde prior to permeabilization and staining with the following antibodies: IL-6-PE, TNF-α-PE/Cy7 (BioLegend), and IL-13-PE (eBioscience).

qRT-PCR

Total RNA was extracted using TRI reagent (MRC) and was retrotranscribed using the qScript cDNA SuperMix kit (Quanta Biosciences). Primer sequences for SYBR Green qRT-PCR and TaqMan primers and probes (Applied Biosystems) are listed in Table S1. The qPCR was performed with an ABI 7900HT Fast Real-Time PCR system (Applied Biosystems). Data analysis was performed using the ΔΔCt method (Livak and Schmittgen, 2001).

Plasmid Construction

Lentiviral vectors were generated using standard cloning techniques. The murine *Cebpa* lentiviral expression vector was purchased from ABM (pLentiGIII-EF1α; NCBI: NM_007678) and either used as is or moved into the pScalps lentiviral vector (Deho' et al., 2014). The murine *Cebpe* gene (NCBI: NM_207131) was cloned by PCR from murine LSK (Lin^{-} Sca1^{+} Kit^{+}) hematopoietic progenitors isolated from the bone marrow. The sequences of shRNAs against murine *Tet3* were as follows: sh1, 5′-CTGTTAGGCAGATTGTTCT; and sh2, 5′-TCCAACGAGAAGCTATTTT. The myc-tagged TET2 carboxy-terminal catalytic DSBH domain with or without substitutions to impair its catalytic activity (TET2 H × D) (Ko et al., 2010) was cloned into the pScalps lentiviral vector. All inserts and mutations were verified by Sanger sequencing.

Lentiviral Transduction

Lentiviral transductions were performed exactly as described (Deho' et al., 2014; Mayoral and Monticelli, 2010). Briefly, viral particles were generated by co-transfection of HEK293T cells with the lentiviral vector together with packaging vectors psPAX2 and pMD2.G (Addgene 12260 and 12259). After concentration by centrifugation, viral particles were added to the cell cultures. Total bone marrow cells were used for most transductions, although in some experiments Lin^{-} hematopoietic precursors were first isolated from the bone marrow using a Lineage Cell Depletion Kit (Miltenyi Biotec). Cells were selected 2–3 days after transduction with 1–2 μg/ml puromycin for 24–48 hr.

Cell Proliferation

Cell proliferation in response to IL-3 was assessed by BrdU incorporation assay exactly as described (Deho' et al., 2014), utilizing an APC-BrdU Flow kit from BD Biosciences. Cells were allowed to incorporate BrdU for 8–12 hr at 37°C.

RNA-Seq

Total RNA (1 μg) was used for mRNA-seq library preparation using the TruSeq RNA Sample Prep kit (Illumina), according to the manufacturer's instructions. Sequencing was performed on a Solexa HiSeq2000 with standard protocols. After quality filtering according to the Illumina pipeline, 51-bp paired-end reads were aligned to the mm9 reference genome, NCBI Build 37, and to the *Mus musculus* transcriptome (University of California, Santa Cruz [UCSC] and Illumina's iGenomes) using TopHat version 1.3.1 (Trapnell et al., 2012). Sequencing statistics for each sample are reported in Table S2. DEGs were identified with Cuffdiff v.2.0.2 (Trapnell et al., 2013) using two biological replicates with the following parameters: minimal FPKM in at least one condition (WT or knockout) ≥ 1; 2-fold in gene expression (WT versus knockout); and p value ≤ 0.05. The complete lists of up- and downregulated genes are provided in Table S3. Identification of enriched GO functional categories in the set of genes up- or downregulated in *Tet2*$^{-/-}$ mast cells was performed with GoTermFinder (p value ≤ 0.01) (Boyle et al., 2004) and REVIGO (Supek et al., 2011). The complete lists of functional categories are provided in Tables S4 and S5. Statistical enrichment of TF consensus DNA-binding sites was scored using PSCAN (Zambelli et al., 2009) and a manually curated library of PWMs as described (Barozzi et al., 2014). The complete lists of over-represented TF subfamilies are provided in Tables S6 and S7.

5hmC Quantification by Dot Blot

Levels of 5hmC were measured exactly as described (Ko et al., 2010; Leoni et al., 2015). Briefly, DNA was isolated with the EZNA Tissue DNA kit (Omega Biotek) and denatured. The 2-fold dilutions, from a starting amount of 100–500 ng, were spotted on a nitrocellulose membrane prior to incubation with an anti-5hmC antibody (Active Motif).

Enrichment-Based Detection of 5hmC

Two independent biological replicates were sequenced by GLIB-seq. Chemical labeling-based 5hmC enrichment was performed utilizing the Hydroxymethyl Collector-seq kit (Active Motif) (Song et al., 2011). Briefly, 4 μg genomic DNA was fragmented to 200–400 bp with a Covaris S2 sonicator (250-bp

protocol for 150 s), purified with 1× AMPure XP beads (Agencourt), and then subjected to biotin-based enrichment of 5hmC. The 5hmC-enriched fragments were processed for Illumina sequencing as described (Garber et al., 2012) with slight modifications (Ostuni et al., 2013).

GLIB-Seq Data Processing and Peak Calling

For each dataset, low-quality reads were filtered out according to the Illumina pipeline, and the remaining reads were mapped to the mouse reference genome mm9 using Bowtie2 (Langmead and Salzberg, 2012), with "very sensitive" preset of parameters. Reads showing multiple mapping and unknown physical and mitochondrial DNA mapping were excluded from further analysis. Duplicate reads were marked and removed using SAMtools (Li et al., 2009). Peaks with significantly enriched signal were called using MACS2 (version 2.1.0.20150731, https://github.com/taoliu/MACS/), with the following added parameters: -g mm -B–SPMR–nomodel–extsize 200 -p 1.00e−04 (Zhang et al., 2008). The direct comparisons $Tet2^{+/+}$ versus $Tet2^{-/-}$ and $Tet2^{-/-}$ versus $Tet2^{+/+}$ were performed with the same parameters. Peaks enriched in $Tet2^{+/+}$ versus $Tet2^{-/-}$ were defined as hypo while regions enriched in $Tet2^{-/-}$ versus $Tet2^{+/+}$ were defined as hyper. Peaks were filtered based on peaks blacklisted by the Encyclopedia of DNA Elements (ENCODE) consortium analysis of artifactual signals in mouse cells (https://sites.google.com/site/anshulkundaje/projects/blacklists). Genome browser tracks were normalized such that each value represents the read per million (RPM) and converted to the bigWig format for visualization on the UCSC Genome Browser using bedGraphToBigWig tool.

Scatterplot of GLIB-Seq Regions

For visualization purposes, all regions identified above were pooled and their coordinates merged in case of overlap. CoverageBed (Quinlan and Hall, 2010) was then used to compute coverage, which was transformed to reads per kilobase per million mapped reads (RPKM) and log2-transformed for each region. R software was used to generate the scatterplot.

Determination of Genomic Localization

The genomic localization of peaks was carried out using *annotatePeaks* (Heinz et al., 2010) based on mm9 RefSeq as reference. We classified peaks as either proximal or distal based on their proximity to TSSs. Proximal peaks were located within ±2.5 kb from the TSS while all other peaks were classified as distal.

Functional Enrichment Analysis

For each list of enriched regions of interest, GREAT 3.0.0 (McLean et al., 2010) was used with default parameters and selecting the whole mm9 genome as background. The complete lists of functional categories are provided in Table S8.

H3K4me1 ChIP-Seq

ChIP-seq was performed as described (Ostuni et al., 2013). The following MACS2 parameters were used: -g mm -B–SPMR–nomodel–extsize 146 -p 1.00e−04.

Statistical Analysis

Statistical analysis was performed with Prism software (GraphPad). Data are represented as mean ± SEM, and significance was assessed by paired or unpaired Student's t test, two-tailed, or two-way ANOVA.

ACCESSION NUMBERS

The accession number for the RNA-seq, GLIB-seq, and ChIP-seq raw datasets reported in this paper is GEO: GSE77845.

SUPPLEMENTAL INFORMATION

Supplemental Information includes six figures and eight tables and can be found with this article online at http://dx.doi.org/10.1016/j.celrep.2016.04.044.

AUTHOR CONTRIBUTIONS

S. Montagner and C.L. designed and performed experiments and analyzed data. S.E., G.D.C., and S.T. performed experiments. C.B., I.B., V.P., and G.N. analyzed data. M.K. and A.R. provided essential reagents and intellectual input. G.N. and S. Monticelli wrote the paper. S. Monticelli designed and supervised the study, analyzed data, and secured funding.

ACKNOWLEDGMENTS

A special thank you to D. Jarrossay for technical assistance, to E. Rugarli for the NSC-34 cell line, and to M. Tahiliani for critical reading of the manuscript. This work was supported by grants from the following to S.M.: Swiss National Science Foundation (156875), San Salvatore Foundation, Novartis Foundation, and Ceresio Foundation.

Received: August 18, 2015
Revised: March 8, 2016
Accepted: April 7, 2016
Published: May 5, 2016; corrected online: August 15, 2017

REFERENCES

Abdel-Wahab, O., Mullally, A., Hedvat, C., Garcia-Manero, G., Patel, J., Wadleigh, M., Malinge, S., Yao, J., Kilpivaara, O., Bhat, R., et al. (2009). Genetic characterization of TET1, TET2, and TET3 alterations in myeloid malignancies. Blood *114*, 144–147.

Amati, B., Frank, S.R., Donjerkovic, D., and Taubert, S. (2001). Function of the c-Myc oncoprotein in chromatin remodeling and transcription. Biochim. Biophys. Acta *1471*, M135–M145.

An, J., González-Avalos, E., Chawla, A., Jeong, M., López-Moyado, I.F., Li, W., Goodell, M.A., Chavez, L., Ko, M., and Rao, A. (2015). Acute loss of TET function results in aggressive myeloid cancer in mice. Nat. Commun. *6*, 10071.

Barozzi, I., Simonatto, M., Bonifacio, S., Yang, L., Rohs, R., Ghisletti, S., and Natoli, G. (2014). Coregulation of transcription factor binding and nucleosome occupancy through DNA features of mammalian enhancers. Mol. Cell *54*, 844–857.

Blaschke, K., Ebata, K.T., Karimi, M.M., Zepeda-Martínez, J.A., Goyal, P., Mahapatra, S., Tam, A., Laird, D.J., Hirst, M., Rao, A., et al. (2013). Vitamin C induces Tet-dependent DNA demethylation and a blastocyst-like state in ES cells. Nature *500*, 222–226.

Boyle, E.I., Weng, S., Gollub, J., Jin, H., Botstein, D., Cherry, J.M., and Sherlock, G. (2004). GO:TermFinder–open source software for accessing Gene Ontology information and finding significantly enriched Gene Ontology terms associated with a list of genes. Bioinformatics *20*, 3710–3715.

Cashman, N.R., Durham, H.D., Blusztajn, J.K., Oda, K., Tabira, T., Shaw, I.T., Dahrouge, S., and Antel, J.P. (1992). Neuroblastoma x spinal cord (NSC) hybrid cell lines resemble developing motor neurons. Dev. Dyn. *194*, 209–221.

Chen, Q., Chen, Y., Bian, C., Fujiki, R., and Yu, X. (2013). TET2 promotes histone O-GlcNAcylation during gene transcription. Nature *493*, 561–564.

De Vita, S., Schneider, R.K., Garcia, M., Wood, J., Gavillet, M., Ebert, B.L., Gerbaulet, A., Roers, A., Levine, R.L., Mullally, A., and Williams, D.A. (2014). Loss of function of TET2 cooperates with constitutively active KIT in murine and human models of mastocytosis. PLoS ONE *9*, e96209.

Deho', L., Leoni, C., Brodie, T.M., Montagner, S., De Simone, M., Polletti, S., Barozzi, I., Natoli, G., and Monticelli, S. (2014). Two functionally distinct subsets of mast cells discriminated By IL-2-independent CD25 activities. J. Immunol. *193*, 2196–2206.

Deplus, R., Delatte, B., Schwinn, M.K., Defrance, M., Méndez, J., Murphy, N., Dawson, M.A., Volkmar, M., Putmans, P., Calonne, E., et al. (2013). TET2 and TET3 regulate GlcNAcylation and H3K4 methylation through OGT and SET1/COMPASS. EMBO J. *32*, 645–655.

Gallant, P., and Steiger, D. (2009). Myc's secret life without Max. Cell Cycle *8*, 3848–3853.

Garber, M., Yosef, N., Goren, A., Raychowdhury, R., Thielke, A., Guttman, M., Robinson, J., Minie, B., Chevrier, N., Itzhaki, Z., et al. (2012). A high-throughput chromatin immunoprecipitation approach reveals principles of dynamic gene regulation in mammals. Mol. Cell *47*, 810–822.

Hahn, M.A., Qiu, R., Wu, X., Li, A.X., Zhang, H., Wang, J., Jui, J., Jin, S.G., Jiang, Y., Pfeifer, G.P., and Lu, Q. (2013). Dynamics of 5-hydroxymethylcytosine and chromatin marks in Mammalian neurogenesis. Cell Rep. *3*, 291–300.

Heintzman, N.D., Stuart, R.K., Hon, G., Fu, Y., Ching, C.W., Hawkins, R.D., Barrera, L.O., Van Calcar, S., Qu, C., Ching, K.A., et al. (2007). Distinct and predictive chromatin signatures of transcriptional promoters and enhancers in the human genome. Nat. Genet. *39*, 311–318.

Heintzman, N.D., Hon, G.C., Hawkins, R.D., Kheradpour, P., Stark, A., Harp, L.F., Ye, Z., Lee, L.K., Stuart, R.K., Ching, C.W., et al. (2009). Histone modifications at human enhancers reflect global cell-type-specific gene expression. Nature *459*, 108–112.

Heinz, S., Benner, C., Spann, N., Bertolino, E., Lin, Y.C., Laslo, P., Cheng, J.X., Murre, C., Singh, H., and Glass, C.K. (2010). Simple combinations of lineage-determining transcription factors prime cis-regulatory elements required for macrophage and B cell identities. Mol. Cell *38*, 576–589.

Hon, G.C., Song, C.X., Du, T., Jin, F., Selvaraj, S., Lee, A.Y., Yen, C.A., Ye, Z., Mao, S.Q., Wang, B.A., et al. (2014). 5mC oxidation by Tet2 modulates enhancer activity and timing of transcriptome reprogramming during differentiation. Mol. Cell *56*, 286–297.

Huang, Y., and Rao, A. (2014). Connections between TET proteins and aberrant DNA modification in cancer. Trends Genet. *30*, 464–474.

Huang, Y., Chavez, L., Chang, X., Wang, X., Pastor, W.A., Kang, J., Zepeda-Martínez, J.A., Pape, U.J., Jacobsen, S.E., Peters, B., and Rao, A. (2014). Distinct roles of the methylcytosine oxidases Tet1 and Tet2 in mouse embryonic stem cells. Proc. Natl. Acad. Sci. USA *111*, 1361–1366.

Ito, S., Shen, L., Dai, Q., Wu, S.C., Collins, L.B., Swenberg, J.A., He, C., and Zhang, Y. (2011). Tet proteins can convert 5-methylcytosine to 5-formylcytosine and 5-carboxylcytosine. Science *333*, 1300–1303.

Iwasaki, H., Mizuno, S., Arinobu, Y., Ozawa, H., Mori, Y., Shigematsu, H., Takatsu, K., Tenen, D.G., and Akashi, K. (2006). The order of expression of transcription factors directs hierarchical specification of hematopoietic lineages. Genes Dev. *20*, 3010–3021.

Ko, M., Huang, Y., Jankowska, A.M., Pape, U.J., Tahiliani, M., Bandukwala, H.S., An, J., Lamperti, E.D., Koh, K.P., Ganetzky, R., et al. (2010). Impaired hydroxylation of 5-methylcytosine in myeloid cancers with mutant TET2. Nature *468*, 839–843.

Ko, M., Bandukwala, H.S., An, J., Lamperti, E.D., Thompson, E.C., Hastie, R., Tsangaratou, A., Rajewsky, K., Koralov, S.B., and Rao, A. (2011). Ten-Eleven-Translocation 2 (TET2) negatively regulates homeostasis and differentiation of hematopoietic stem cells in mice. Proc. Natl. Acad. Sci. USA *108*, 14566–14571.

Ko, M., An, J., Pastor, W.A., Koralov, S.B., Rajewsky, K., and Rao, A. (2015). TET proteins and 5-methylcytosine oxidation in hematological cancers. Immunol. Rev. *263*, 6–21.

Langmead, B., and Salzberg, S.L. (2012). Fast gapped-read alignment with Bowtie 2. Nat. Methods *9*, 357–359.

Leoni, C., Montagner, S., Deho', L., D'Antuono, R., De Matteis, G., Marzano, A.V., Merante, S., Orlandi, E.M., Zanotti, R., and Monticelli, S. (2015). Reduced DNA methylation and hydroxymethylation in patients with systemic mastocytosis. Eur. J. Haematol. *95*, 566–575.

Li, H., Handsaker, B., Wysoker, A., Fennell, T., Ruan, J., Homer, N., Marth, G., Abecasis, G., and Durbin, R.; 1000 Genome Project Data Processing Subgroup (2009). The Sequence Alignment/Map format and SAMtools. Bioinformatics *25*, 2078–2079.

Livak, K.J., and Schmittgen, T.D. (2001). Analysis of relative gene expression data using real-time quantitative PCR and the 2(-Delta Delta C(T)) Method. Methods *25*, 402–408.

Lu, F., Liu, Y., Jiang, L., Yamaguchi, S., and Zhang, Y. (2014). Role of Tet proteins in enhancer activity and telomere elongation. Genes Dev. *28*, 2103–2119.

Mayoral, R.J., and Monticelli, S. (2010). Stable overexpression of miRNAs in bone marrow-derived murine mast cells using lentiviral expression vectors. Methods Mol. Biol. *667*, 205–214.

Mayoral, R.J., Deho, L., Rusca, N., Bartonicek, N., Saini, H.K., Enright, A.J., and Monticelli, S. (2011). MiR-221 influences effector functions and actin cytoskeleton in mast cells. PLoS ONE *6*, e26133.

McLean, C.Y., Bristor, D., Hiller, M., Clarke, S.L., Schaar, B.T., Lowe, C.B., Wenger, A.M., and Bejerano, G. (2010). GREAT improves functional interpretation of cis-regulatory regions. Nat. Biotechnol. *28*, 495–501.

Ostuni, R., Piccolo, V., Barozzi, I., Polletti, S., Termanini, A., Bonifacio, S., Curina, A., Prosperini, E., Ghisletti, S., and Natoli, G. (2013). Latent enhancers activated by stimulation in differentiated cells. Cell *152*, 157–171.

Pastor, W.A., Aravind, L., and Rao, A. (2013). TETonic shift: biological roles of TET proteins in DNA demethylation and transcription. Nat. Rev. Mol. Cell Biol. *14*, 341–356.

Paul, F., Arkin, Y., Giladi, A., Jaitin, D.A., Kenigsberg, E., Keren-Shaul, H., Winter, D., Lara-Astiaso, D., Gury, M., Weiner, A., et al. (2015). Transcriptional Heterogeneity and Lineage Commitment in Myeloid Progenitors. Cell *163*, 1663–1677.

Qi, X., Hong, J., Chaves, L., Zhuang, Y., Chen, Y., Wang, D., Chabon, J., Graham, B., Ohmori, K., Li, Y., and Huang, H. (2013). Antagonistic regulation by the transcription factors C/EBPα and MITF specifies basophil and mast cell fates. Immunity *39*, 97–110.

Quinlan, A.R., and Hall, I.M. (2010). BEDTools: a flexible suite of utilities for comparing genomic features. Bioinformatics *26*, 841–842.

Rasmussen, K.D., Jia, G., Johansen, J.V., Pedersen, M.T., Rapin, N., Bagger, F.O., Porse, B.T., Bernard, O.A., Christensen, J., and Helin, K. (2015). Loss of TET2 in hematopoietic cells leads to DNA hypermethylation of active enhancers and induction of leukemogenesis. Genes Dev. *29*, 910–922.

Ren, B., Cam, H., Takahashi, Y., Volkert, T., Terragni, J., Young, R.A., and Dynlacht, B.D. (2002). E2F integrates cell cycle progression with DNA repair, replication, and G(2)/M checkpoints. Genes Dev. *16*, 245–256.

Rishi, V., Bhattacharya, P., Chatterjee, R., Rozenberg, J., Zhao, J., Glass, K., Fitzgerald, P., and Vinson, C. (2010). CpG methylation of half-CRE sequences creates C/EBPalpha binding sites that activate some tissue-specific genes. Proc. Natl. Acad. Sci. USA *107*, 20311–20316.

Rusca, N., Dehò, L., Montagner, S., Zielinski, C.E., Sica, A., Sallusto, F., and Monticelli, S. (2012). MiR-146a and NF-κB1 regulate mast cell survival and T lymphocyte differentiation. Mol. Cell. Biol. *32*, 4432–4444.

Song, C.X., Szulwach, K.E., Fu, Y., Dai, Q., Yi, C., Li, X., Li, Y., Chen, C.H., Zhang, W., Jian, X., et al. (2011). Selective chemical labeling reveals the genome-wide distribution of 5-hydroxymethylcytosine. Nat. Biotechnol. *29*, 68–72.

Soucie, E., Hanssens, K., Mercher, T., Georgin-Lavialle, S., Damaj, G., Livideanu, C., Chandesris, M.O., Acin, Y., Létard, S., de Sepulveda, P., et al. (2012). In aggressive forms of mastocytosis, TET2 loss cooperates with c-KITD816V to transform mast cells. Blood *120*, 4846–4849.

Spruijt, C.G., Gnerlich, F., Smits, A.H., Pfaffeneder, T., Jansen, P.W., Bauer, C., Münzel, M., Wagner, M., Müller, M., Khan, F., et al. (2013). Dynamic readers for 5-(hydroxy)methylcytosine and its oxidized derivatives. Cell *152*, 1146–1159.

Supek, F., Bošnjak, M., Škunca, N., and Šmuc, T. (2011). REVIGO summarizes and visualizes long lists of gene ontology terms. PLoS ONE *6*, e21800.

Tahiliani, M., Koh, K.P., Shen, Y., Pastor, W.A., Bandukwala, H., Brudno, Y., Agarwal, S., Iyer, L.M., Liu, D.R., Aravind, L., and Rao, A. (2009). Conversion of 5-methylcytosine to 5-hydroxymethylcytosine in mammalian DNA by MLL partner TET1. Science *324*, 930–935.

Theoharides, T.C., Valent, P., and Akin, C. (2015). Mast Cells, Mastocytosis, and Related Disorders. N. Engl. J. Med. *373*, 163–172.

Trapnell, C., Roberts, A., Goff, L., Pertea, G., Kim, D., Kelley, D.R., Pimentel, H., Salzberg, S.L., Rinn, J.L., and Pachter, L. (2012). Differential gene and transcript expression analysis of RNA-seq experiments with TopHat and Cufflinks. Nat. Protoc. *7*, 562–578.

Trapnell, C., Hendrickson, D.G., Sauvageau, M., Goff, L., Rinn, J.L., and Pachter, L. (2013). Differential analysis of gene regulation at transcript resolution with RNA-seq. Nat. Biotechnol. *31*, 46–53.

Tsai, M., Takeishi, T., Thompson, H., Langley, K.E., Zsebo, K.M., Metcalfe, D.D., Geissler, E.N., and Galli, S.J. (1991). Induction of mast cell proliferation, maturation, and heparin synthesis by the rat c-kit ligand, stem cell factor. Proc. Natl. Acad. Sci. USA *88*, 6382–6386.

Williams, K., Christensen, J., Pedersen, M.T., Johansen, J.V., Cloos, P.A., Rappsilber, J., and Helin, K. (2011). TET1 and hydroxymethylcytosine in transcription and DNA methylation fidelity. Nature *473*, 343–348.

Wu, H., D'Alessio, A.C., Ito, S., Xia, K., Wang, Z., Cui, K., Zhao, K., Sun, Y.E., and Zhang, Y. (2011). Dual functions of Tet1 in transcriptional regulation in mouse embryonic stem cells. Nature *473*, 389–393.

Yamanaka, R., Barlow, C., Lekstrom-Himes, J., Castilla, L.H., Liu, P.P., Eckhaus, M., Decker, T., Wynshaw-Boris, A., and Xanthopoulos, K.G. (1997). Impaired granulopoiesis, myelodysplasia, and early lethality in CCAAT/enhancer binding protein epsilon-deficient mice. Proc. Natl. Acad. Sci. USA *94*, 13187–13192.

Yin, R., Mao, S.Q., Zhao, B., Chong, Z., Yang, Y., Zhao, C., Zhang, D., Huang, H., Gao, J., Li, Z., et al. (2013). Ascorbic acid enhances Tet-mediated 5-methylcytosine oxidation and promotes DNA demethylation in mammals. J. Am. Chem. Soc. *135*, 10396–10403.

Yue, X., Trifari, S., Äijö, T., Tsagaratou, A., Pastor, W.A., Zepeda-Martínez, J.A., Lio, C.W., Li, X., Huang, Y., Vijayanand, P., et al. (2016). Control of Foxp3 stability through modulation of TET activity. J. Exp. Med. *213*, 377–397.

Zambelli, F., Pesole, G., and Pavesi, G. (2009). Pscan: finding over-represented transcription factor binding site motifs in sequences from co-regulated or co-expressed genes. Nucleic Acids Res. *37*, W247–252.

Zhang, Y., Liu, T., Meyer, C.A., Eeckhoute, J., Johnson, D.S., Bernstein, B.E., Nusbaum, C., Myers, R.M., Brown, M., Li, W., and Liu, X.S. (2008). Model-based analysis of ChIP-Seq (MACS). Genome Biol. *9*, R137.

Zhang, Q., Zhao, K., Shen, Q., Han, Y., Gu, Y., Li, X., Zhao, D., Liu, Y., Wang, C., Zhang, X., et al. (2015). Tet2 is required to resolve inflammation by recruiting Hdac2 to specifically repress IL-6. Nature *525*, 389–393.

Cell Reports, Volume *15*

Supplemental Information

TET2 Regulates Mast Cell Differentiation and Proliferation through Catalytic and Non-catalytic Activities

Sara Montagner, Cristina Leoni, Stefan Emming, Giulia Della Chiara, Chiara Balestrieri, Iros Barozzi, Viviana Piccolo, Susan Togher, Myunggon Ko, Anjana Rao, Gioacchino Natoli, and Silvia Monticelli

Supplemental Information

Supplemental Data

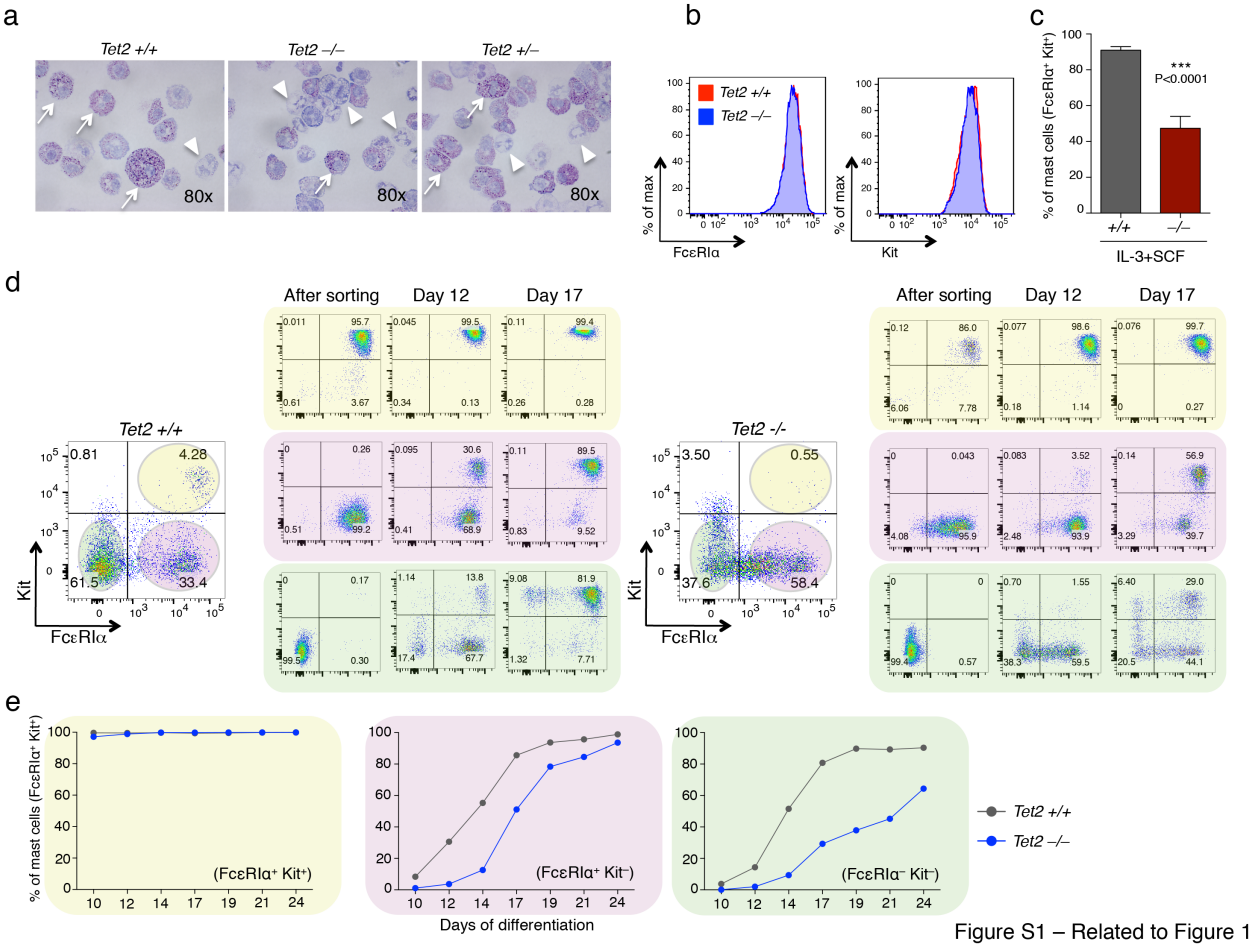

Figure S1 – Related to Figure 1

Supplemental Figure S1 – Related to Figure 1. Delayed mast cell differentiation in the absence of *Tet2*. (a) Cells were cytospun on a glass slide and stained with Toluidine blue exactly as described (Mayoral and Monticelli, 2010). Arrows indicate mast cells, characterized by purple cytoplasmic granules, and arrowheads non-mast cells. **(b)** *Tet2*+/+ and *Tet2*-/- bone marrow cells were *in vitro* differentiated in presence of IL-3 for four weeks; levels of surface expression of the mast cell markers FcεRIα and Kit were assessed by flow cytometry. **(c)** *Tet2*+/+ and *Tet2*-/- bone marrow cells were *in vitro* differentiated in presence of IL-3 and 5-20ng/mL murine SCF (Peprotech) for 2.5 weeks. The percentage of mast cells ($FcεRIα^+$ Kit^+ cells) in culture was assessed by surface staining and flow cytometry analysis. Shown are the compiled results of two independent experiments, each performed in triplicate. **(d-e)** Bone marrow cells were differentiated in culture for 10 days prior staining and separation by cell-sorting in the three indicated sub-populations, namely $Kit^{–/lo}$ $FcεRIα^–$ precursors (green), the intermediate GMP stage (pink), and differentiated mast cells (yellow). Two days after sorting (day 12 of differentiation), and then every 2-3 days until day 24 of differentiation, cultures were evaluated for the percentage of differentiated mast cells.

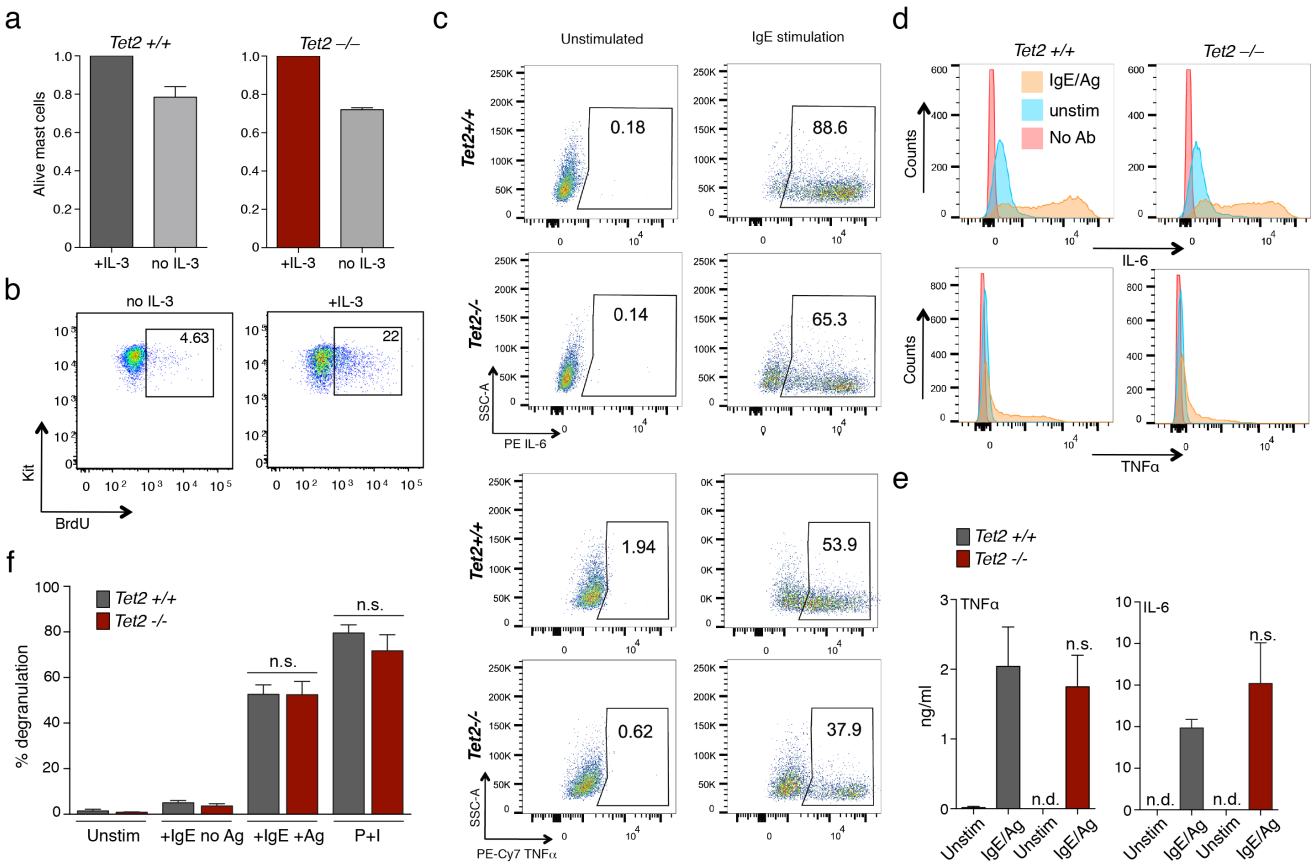

Supplemental Figure S2 – Related to Figure 1. Reduced cytokine production, normal survival and degranulation in mast cells lacking *Tet2*. **(a)** Cell death in response to prolonged withdrawal of IL-3 is not influenced by *Tet2* deletion. Cells were deprived of IL-3 for three days prior staining for Kit (to detect mast cells) and Aqua Dead dye (LIVE/DEAD Fixable Aqua Dead Cell Stain Kit, Life Technologies). Shown is the amount of live mast cells (Kit^+ Aqua $Dead^-$) in the absence of IL-3 relative to their controls (+IL-3 conditions). Cell viability was reduced by less than 30% upon withdrawal of survival factors, regardless of TET2 expression. Shown are the compiled results of two independent experiments. **(b)** Mast cell proliferation is dependent on IL-3. IL-3 was withdrawn for the culture O/N (no cell death is normally detected after such a short time of starvation, as we previously showed (Rusca et al., 2012)) or re-added prior to BrdU incorporation and analysis of proliferation. **(c)** Mast cells were either left unstimulated or were stimulated for 3h with IgE and antigen prior fixation, permeabilization and intracellular cytokine staining. A representative staining is shown for IL-6 and TNFα. **(d)** Same as (c), showing also the no-antibody control stainings, revealing no significant differences between *Tet2-/-* and *Tet2+/+* unstimulated cells. **(e)** Mast cells were left unstimulated or were stimulated for 12h with IgE and antigen prior analysis of cytokine accumulation in the cell supernatant by ELISA following exactly manufacturer's instructions (Mouse High Sensitivity ELISA, eBioscience). N=3, mean ± SEM; n.d.: undetectable. **(f)** The percentage of mast cell degranulation was measured by β-hexosaminidase enzymatic assay, performed exactly as described (Mayoral et al., 2011). Briefly, the degranulation capacity was assessed by measuring the release in the supernatant of β-hexosaminidase (an enzyme normally contained in the cytoplasmic granules) upon stimulation. Cells were either left unstimulated, treated with IgE but with no addition of antigen, fully stimulated with IgE and antigen, or with PMA and ionomycin as a positive control (N=4, mean ± SEM).

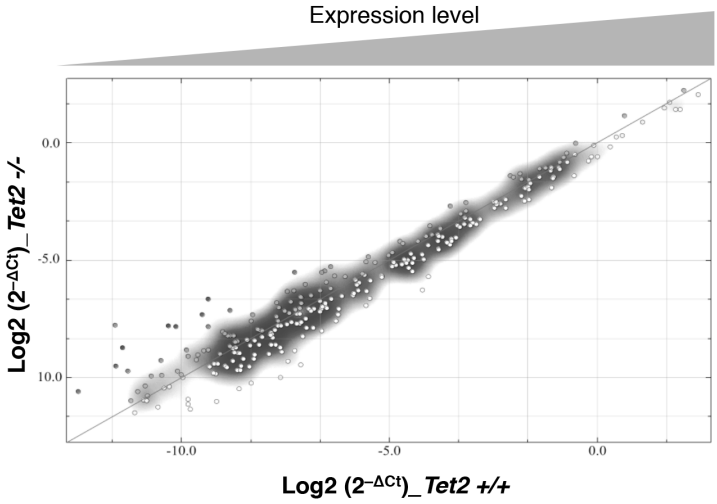

Supplemental Figure S3 – Related to Figures 2. Analysis of miRNA expression in mast cells. To describe the miRnome of *Tet2*+/+ and *Tet2*–/– mast cells, cells were first separated at ≥ 95% purity by sorting FcεRIα^{+} Kit^{+} cells, prior to total RNA extraction and qRT-PCR utilizing the Ready-to-Use PCR Mouse & Rat Panel I + II V3 (Exiqon). This system allows profiling of 742 different miRNAs in 384-well plates format. Retrotranscription and qPCR were performed following exactly manufacturer's instructions. To correct for variability due to different PCR runs, an interplate calibrator was used as recommended by the manufacturer. MiRNAs with Ct values ≥35 were considered as undetected and excluded from further analysis, and only miRNAs with Cts reproducibly <35 in at least two out three replicates were further processed. MiRNA expression was normalized to different endogenous controls (RNU1A1, RNU5G and U6 snRNA) to obtain the ΔCts and the $2^{-\Delta Ct}$ values were finally plotted. Statistic was performed using an unpaired Student t-test and global data visualization was performed with J-Express software (Dysvik and Jonassen, 2001).

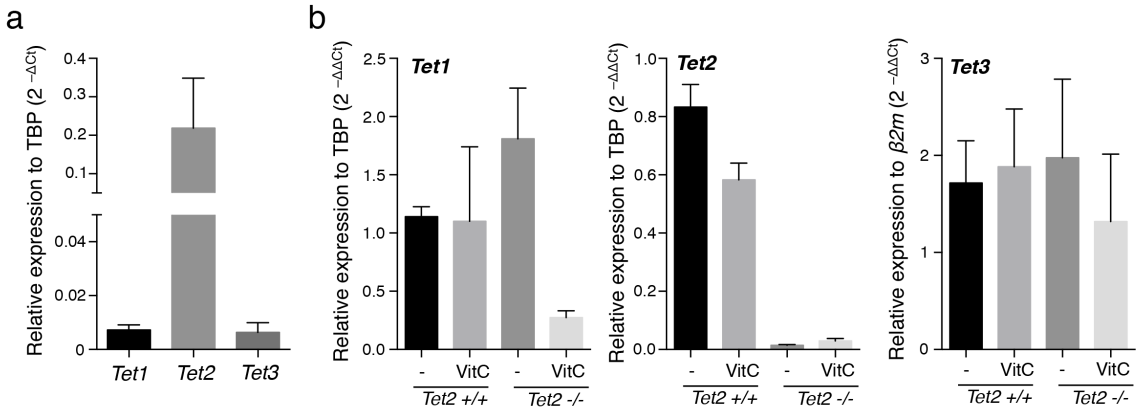

Supplemental Figure S4 – Related to Figures 3. Analysis of *Tet1-3* mRNA expression in mast cells. **(a)** Expression of the different *Tet* mRNAs was assessed by qRT-PCR (primer sequences are indicated in the Supplemental Table S1). Expression was normalized to *Tbp*, used as endogenous control. Shown are the compiled results of four independent experiments. **(b)** *Tet2*+/+ and *Tet2*-/- mast cells were treated for 10 days with 50 μg/ml vitamin C prior RNA extraction and analysis of *Tet* mRNAs expression by either SYBR green (probes indicated in the Supplemental Table S1) or TaqMan based qRT-PCR (specifically for TET3, probes purchased from Applied Biosystem). Shown are the compiled results of four independent experiments, mean ± SEM.

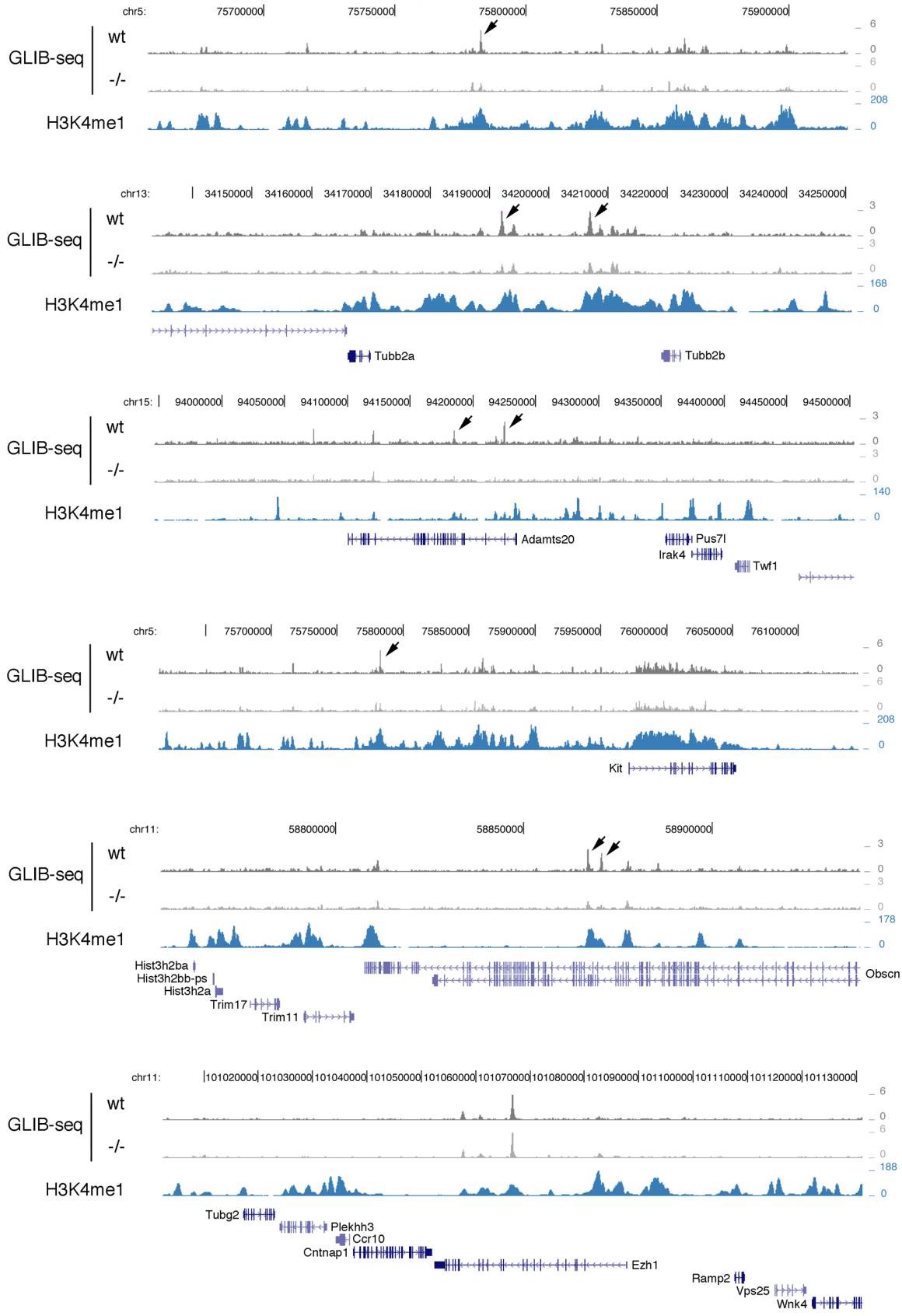

Supplemental Figure S5 – Related to Figures 7. Illustrative snapshots of GLIB-seq data. Illustrative snapshots of GLIB-seq and H3K4me1 ChIP-seq data presented in Figure 7. Arrows indicate regions with loss if hydroxymethylation, which for the most part, coincided with peaks of H3K4me1 modification. The bottom last genomic region is an example of an area with no changes in hydroxymethylation.

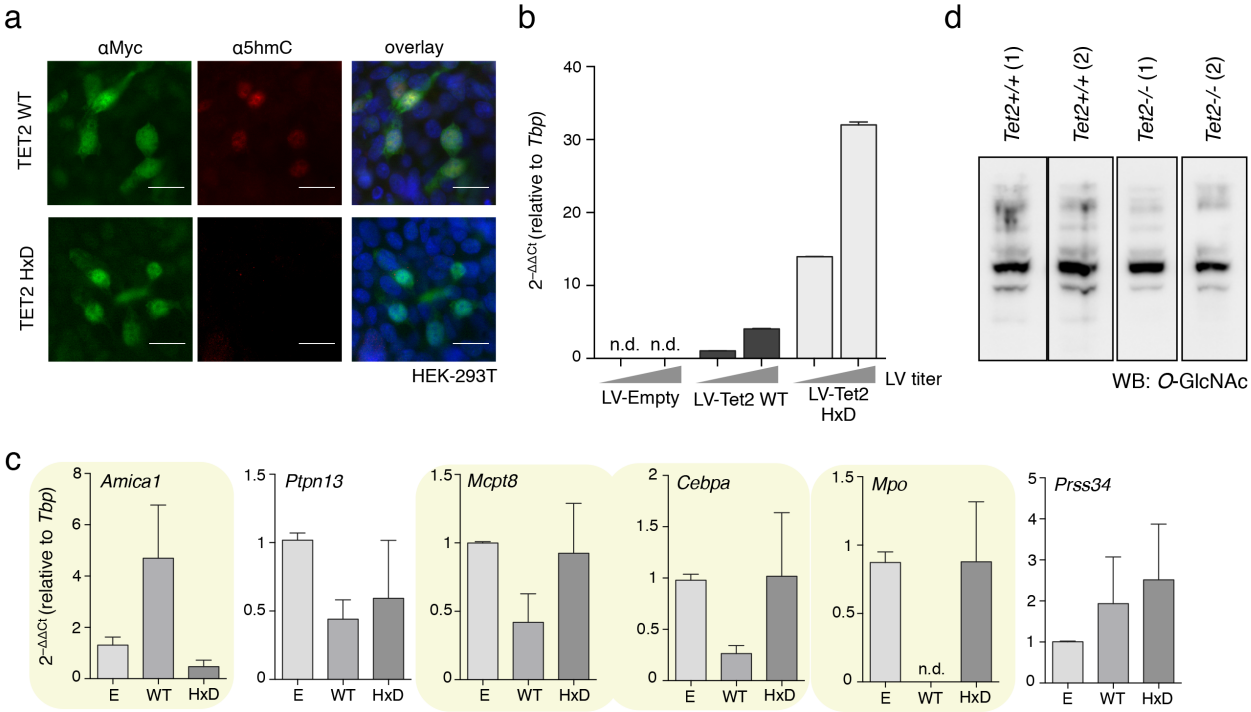

Supplemental Figure S6 – Related to Figures 7. Expression and functionality of the catalytic domain of wild-type or mutated (HxD) TET2. (a) Immunofluorescence experiments were performed exactly as described (Leoni et al., 2015). Briefly, HEK-293T cells were transfected with Lipofectamine 2000 (LifeTechnologies) following exactly manufacturer's instructions. Transfected HEK-293T cells were fixed with 4% paraformaldehyde for 15 min and permeabilized with 0.2% Triton X-100 for 15 min. To denature the DNA, cells were treated with 2N HCl for 30 min, followed by neutralization with 100 mM Tris-HCl buffer (pH 8.0). After blocking with 1% BSA, cells were stained with mouse anti-5hmC (Active Motif) and rabbit anti-myc (Sigma) antibodies. Nuclei were counterstained with DAPI. For microscope image acquisition, a Nikon Eclipse E800 upright microscope was used, and images were acquired with an EM-CCD camera (Hamamatsu Digital Camera C9100), using the acquisition software VisiView (Visitron System GmbH) Version 2.0.8. The scale bar represents 25µm. **(b)** *Tet2-/-* mast cells were transduced with the indicated lentiviral vectors. After selection with puromycin, the expression of the *Tet2* mRNA was assessed by SYBR green qRT-PCR (probes indicated in the Supplemental Table S1). Shown is one representative experiment of three. **(c)** Same as in (b), except that the expression of the indicated genes was assessed. Yellow shading highlights the genes whose expression was rescued by the reconstitution with TET2 WT, but not with mutated TET2. Shown is the expression relative to *Tbp* (endogenous control) and to the control vector; N=5, mean ± SEM. n.d.: undetectable. E=empty vector; WT=TET2 WT vector; HxD=TET2 HxD mutated vector. **(d)** *Tet2*+/+ and *Tet2-/-* mast cells derived from two independent animals (1 and 2) were lysed in RIPA buffer and Western blot was performed with an anti-*O*-GlcNAc antibody (*O*-linked N-acetylglucosamine antibody (RL2), Thermo Scientific).

Supplemental Table S1. Primers used in qRT-PCR, Related to Figures 3, 5, 6

Sybr Green primers		
Gene name	**Primer FW**	**Primer RV**
Mpo	5'-AGATGAAGCTACTCTTGGCCTTGGC-3'	5'-GCTCCTTGTAGGCTCTGTCCACTAGC-3'
Cebpa	5'-GTGGACAAGAACAGCAACGAG-3'	5'-TCACTGGTCAACTCCAGCAC-3'
Mcpt8	5'-ACAACGACTCCATCCAGCTC-3'	5'-CACAAGCGACAACTGACAATGC-3'
Prss34	5'-GTTGTGCTGTCTGAGCATGTCTACC-3'	5'-GAAGAATTGGTCTGGTACTTCTGCTCA-3'
Amica1	5'-CTAAAGATCTCAGAGTCCGAGTAGGTG-3'	5'-GCATGTTGGAGTCATAGCTCAAGA-3'
Ptpn13	5'-GGCCAGACACGACCAAGTAGAC-3'	5'-CTAGAGATGTCGAGCATGGAAGC-3'
Cebpe	5'-CAGCCCTTGCGTGTCCTCAAG-3'	5'-CTTTGTTCACTGCCTTCTTGCCC-3'
Tet1	5'-GGAATGAGTTCTGAAGGAAGTGACGTG-3'	5'-CCAGCAACTTCTTCATATTCCACCTGA-3'
Tet2	5'-AACCTGGCTACTGTCATTGCTCCA-3'	5'-AGCAGAGAAGTCCAAACATGCAGTG-3'
Tet3	5'-ACAAGGACCAACATAACCTCTACAATGG-3'	5'-CCACTACTGACCTTGGCGTTCTG-3'
Endogenous control		
Tbp	5'-CTGGAATTGTACCGCAGCTT-3'	5'-ATGATGACTGCAGCAAATCG-3'

Taqman probes	
Gene name	**Probe number**
Tet1	Mm01169087_m1
Tet2	Mm01312907_m1
Tet3	Mm00805756_m1
Endogenous control	
β2m	Mm00437762_m1

Supplemental Table S2. Statistics for each RNA-seq sample, Related to Figure 2.

Sample	Mapped reads	Properly paired reads
Tet2−/−_m1	104,184,824	86,358,252
Tet2−/−_m2	99,220,872	88,963,880
Tet2+/+_m1	80,741,743	65,520,248
Tet2+/+_m2	90,700,488	76,350,024

Supplemental References

Dysvik, B., and Jonassen, I. (2001). J-Express: exploring gene expression data using Java. Bioinformatics *17*, 369-370.

Leoni, C., Montagner, S., Deho, L., D'Antuono, R., De Matteis, G., Marzano, A.V., Merante, S., Orlandi, E.M., Zanotti, R., and Monticelli, S. (2015). Reduced DNA methylation and hydroxymethylation in patients with systemic mastocytosis. European journal of haematology.

Mayoral, R.J., Deho, L., Rusca, N., Bartonicek, N., Saini, H.K., Enright, A.J., and Monticelli, S. (2011). MiR-221 influences effector functions and actin cytoskeleton in mast cells. PloS one *6*, e26133.

Mayoral, R.J., and Monticelli, S. (2010). Stable overexpression of miRNAs in bone marrow-derived murine mast cells using lentiviral expression vectors. Methods in molecular biology *667*, 205-214.

Rusca, N., Deho, L., Montagner, S., Zielinski, C.E., Sica, A., Sallusto, F., and Monticelli, S. (2012). MiR-146a and NF-kappaB1 regulate mast cell survival and T lymphocyte differentiation. Molecular and cellular biology *32*, 4432-4444.